Journal of Hazardous Materials 422 (2022) 126950

Contents lists available at ScienceDirect

Journal of Hazardous Materials

journal homepage: www.elsevier.com/locate/jhazmat

Review

Recent progress of noble metals with tailored features in catalytic oxidation for organic pollutants degradation

Yukui Fu [a,1], Zhuo Yin [b,1], Lei Qin [a], Danlian Huang [a], Huan Yi [a], Xigui Liu [a], Shiyu Liu [a], Mingming Zhang [a], Bisheng Li [a], Ling Li [a], Wenjun Wang [a], Xuerong Zhou [a], Yixia Li [a], Guangming Zeng [a,b,*], Cui Lai [a,**]

[a] College of Environmental Science and Engineering and Key Laboratory of Environmental Biology and Pollution Control (Ministry of Education), Hunan University, Changsha 410082, PR China
[b] Department of Urology, Second Xiangya Hospital, Central South University, Changsha 410011, PR China

ARTICLE INFO

Editor: Dr. L. Haizhou

Keywords:
Noble metals
Tailored features
Oxidation degradation
Organic pollutants

ABSTRACT

With the increasing serious water pollutions, an increasing interest has given for the nanocomposites as environmental catalysts. To date, noble metals-based nanocomposites have been extensively studied by researchers in environmental catalysis. In detail, serving as key functional parts, noble metals are usually combined with other nanomaterials for rationally designing nanocomposites, which exhibit enhanced catalytic properties in pollutants removal. Noble metals in the nanocomposites possess tailored properties, thus playing different important roles in catalytic oxidation reactions for pollutants removal. To motivate the research and elaborate the progress of noble metals, this review (i) summarizes advanced characterization techniques and rising technology of theoretical calculation for evaluating noble metal, and (ii) classifies the roles according to their disparate mechanism in different catalytic oxidation reactions. Meanwhile, the enhanced mechanism and influence factors are discussed. (iii) The conclusions, facing challenges and perspectives are proposed for further development of noble metals-based nanocomposites as environmental catalysts.

1. Introduction

Since the sustainable economic development, global population growth and climate change, various organic pollutants discharges massively into environmental water, thus causing serious environmental pollution and bringing threats towards human health (Chen et al., 2019c; Gautam et al., 2019; Ibrahim et al., 2020; Li et al., 2020b; Liu et al., 2019e; Luo et al., 2020a; Shen et al., 2019a; Song et al., 2020a; Yang et al., 2019c; Ye et al., 2019b). Hence, it is urgent to treat organic pollutants. To date, nanomaterials, with high surface area, abundant active atoms that possess dangling bonds exposed on the surface, have obtained much interesting and provided a great potential as environmental catalyst, which exhibits high catalytic degradation efficiency for organic pollutants (Chen et al., 2019d; Hodges et al., 2018; Luo et al., 2020b; Song et al., 2021; Wang et al., 2020, 2019d; Yang et al., 2020a, 2020c). For most nanomaterials, the key criterion for serving as environmental catalysts is high catalytic activity for rapidly producing reactive oxygen species (ROS) (Yang et al., 2020e; Zhu et al., 2020).

Among the variety of nanomaterials, noble metals (Au, Ag, Pt and Pd) nanomaterials possess high specific surface area, unique electronic and optical properties such as localized surface plasmon resonance (LSPR), which makes up of collective oscillations of free electrons in noble metal NPs driven by the electromagnetic field of incident light, thus exhibiting high catalytic activity for rapidly producing ROS (Huang et al., 2020b; Liotta et al., 2009; Yu et al., 2013; Zhang et al., 2020). For most noble metals nanomaterials, although possessing superior catalytic property, it tends to aggregate to nanoparticles (NPs) with large size, thus decreasing the surface energy, and reducing the lifetime and efficiency (Fu et al., 2019c; Shen et al., 2020). The high cost of noble metals also confines their further applications. Hence, most studies have

* Corresponding author at: College of Environmental Science and Engineering and Key Laboratory of Environmental Biology and Pollution Control(Ministry of Education), Hunan University, Changsha 410082, PR China.
** Corresponding author.
E-mail addresses: zgming@hnu.edu.cn (G. Zeng), laicui@hnu.edu.cn (C. Lai).
[1] These authors contribute equally to this article.

https://doi.org/10.1016/j.jhazmat.2021.126950
Received 23 February 2021; Received in revised form 10 August 2021; Accepted 16 August 2021
Available online 18 August 2021

rationally designed nanocomposites with noble metals as key functional parts, which can realize high activity in catalytic oxidation degradation of pollutants, meanwhile addressing issues and challenges faced by noble metals catalysts (Qin et al., 2019a, 2019c; Zheng et al., 2020). In detail, noble metals in nanocomposites possess tailored properties, which play important roles in different catalytic oxidation reactions for pollutants removal. For instance, noble metals combined with carbon nanomaterials, such as carbon nanotubes and graphene, can realize the precise control of size and morphology related to light absorption ability by engineering noble metals NPs nucleation and growth, and prevent noble metals from aggregation and leaching, thereby realizing high catalytic performance in pollutants degradation (Bogireddy et al., 2020; Cheng et al., 2015, 2020; Teixeira et al., 2018; Wu et al., 2011). Except carbon nanomaterials, noble metals have also combined with other nanomaterials such as metals organic frameworks (MOFs), covalent organic frameworks (COFs) and metal oxides for the photo/Fenton catalytic degradation of pollutants (Hu et al., 2020; Liu et al., 2017b; Misra et al., 2020; Yang et al., 2017, 2019a; Zhou et al., 2018).

In recent years, the publications about the synthesis approach for fabricating noble metal-based nanocomposites and their applications in catalysis have been reported (Ayati et al., 2014; Kavitha et al., 2020; Liu et al., 2019a, 2017a, 2017b; Yang et al., 2019a). For example, Ayati et al. kept an eye on Au NPs/TiO_2 on the catalytic and photocatalytic application for various pollutants removal from wastewater. They discussed the effects of operating parameters such as Au NPs size, loading amount, pH and calcination when synthesizing Au NPs/TiO_2 (Ayati et al., 2014). Liu et al. overviewed the light absorption of metal NPs and mechanisms in metal-induced photocatalysis, and divided the roles of metal NPs into activity enhancement, semiconductors photosensitization, LSPR catalysis, photothermal effect, light-trapping effect in the applications of water splitting, artificial photosynthesis and inert molecular activation (Liu et al., 2017a). And Lin et al. concluded nanohybrids composed of noble metals and metal oxides for some typical solar energy conversion applications, such as photocatalytic degradation of organic pollutants, hydrogen generation, and CO_2 reduction (Liu et al., 2017b). Recently, Kavitha et al. focused on the noble metals-polymeric g-C_3N_4 heterostructure with highlighting the metal deposition methods and optical properties. They discussed the photocatalytic applications according to different noble metals (Ag, Pd, Au and Pt) depositing g-C_3N_4 (Kavitha et al., 2020). It can be known that these present reviews on environmental catalysis application of noble metals-based nanocomposites mostly focused on photocatalytic degradation, and usually emphasized the functions and applications of the holistic nanocomposites. But the systematic summarization for revealing noble metals in the nanocomposites is brief, and the enhanced mechanism for pollutants degradation over noble metals need to be specifically analyzed. In addition, the advanced characterization techniques and theoretical calculation for evaluating noble metals were not specifically concluded.

From current researches of noble metal-based nanocomposites, except for in photocatalysis application, noble metals-based catalysts can be used as multifunctional catalysts in Fenton-like applications to efficiently decompose H_2O_2 to produce •OH, increase the metal redox cycle, or produce H_2O_2 in-situ to reduce the risk in transportation and addition of H_2O_2 (Jiang et al., 2017; Luo et al., 2014; Navalon et al., 2011; Navalon et al., 2010). Hence, the applications of noble metals-based nanocomposites in Fenton-like reactions are worth reviewing. At present, except above mentioned reviews involving photocatalytic applications, some other reviews related to noble metals-based nanocomposites overviewed the synthesis nanocomposites composed of noble metals and other nanomaterials such as zeolite, metal-organic frameworks, magnetic (Fe_3O_4) in other different catalysis applications (Mishra et al., 2019; Wu et al., 2019b; Yang et al., 2017). But few reviews pay attention to noble metals-based nanocomposites for Fenton-like applications. Overall, even if some reviews have already involved the roles of noble metals in nanocomposite for photocatalytic degradation applications, it is not comprehensive and does not refer to the roles of noble metals for Fenton-like reaction applications. An update on the development of noble metals-based nanocomposites in catalytic oxidation degradation of pollutants is relatively absent. Certainly, a systematic conclusion on the underlying mechanism of enhanced catalytic activity is in demand to explore the correlation between degradation activity and roles of noble metals.

This timely review innovatively classifies the roles of noble metals corresponding to different reactions. Specifically, we focus on the recent progress of noble metals in nanocomposites in catalytic oxidation degradation of pollutants (photocatalytic and Fenton/Fenton like oxidation degradation), and classifies the roles according to their disparate role in different catalytic oxidation reactions. In addition, the advanced characterization techniques and rising technology of theoretical calculation for evaluating noble metals, and the facing challenges of noble metals-based nanocomposites as environmental catalysts for further advances are also systematically summarized. The summary will be beneficial to better understand the mechanism, fully utilize the noble metals and promote their catalytic performance in environmental catalysis. In addition, a number of reviews related to noble metals in environmental detection and catalytic reduction of pollutants have been reported by our groups, which impels us to further review the applications and mechanism of noble metals in catalytic degradation of pollutants for fully revealing the progress and achievement of noble metals-based nanomaterials (Fu et al., 2020; He et al., 2020, 2018; Qin et al., 2021, 2018, 2019b).

2. The roles of noble metals in photocatalytic oxidation

Photocatalytic oxidation as one technology of AOPs could realize high removal efficiency of pollutants from wastewater (Lai et al., 2019; Li et al., 2020a; Liu et al., 2020b; Wang et al., 2019c, 2021; Ye et al., 2019a; Yi et al., 2019; Zhou et al., 2020a). However, the disadvantages of commonly used semiconductor-based photocatalysts, such as fast recombination of charge carriers, narrow light response range and photo-corrosion, limit the wide applications of photocatalytic oxidation in environmental pollutant treatment (Li et al., 2019a; Yang et al., 2019b). Up to now, a large number of studies have studying the deposition or doped of noble metals on photocatalysts (Jiang et al., 2015; Wu et al., 2013; Yan et al., 2013), for realizing an enhanced light absorption ability, promoted charge separation and more active sites (Meng et al., 2019a). In this section, the enhanced mechanisms by noble metals in photocatalytic pollutants oxidation are discussed in detail and disparate roles of noble metals are concluded. Moreover, the effect of size, morphology and interface properties is also elaborated by investigation of photocatalytic degradation applications. For comparison, Table 1 lists the photocatalytic pollutant degradation over different noble metals-based nanocomposites according to their disparate role.

2.1. Co-catalyst as light harvesting units

It is well known that maximum harvest and utilization of solar light plays a vital role in promoting photocatalytic activity of photocatalysts. So far, the LSPR of noble metals (Au and Ag), made up of collective oscillations of free electrons in noble metal NPs driven by the electromagnetic field of incident light (Chen et al., 2013a; Fuku et al., 2013; Ma et al., 2018; Zhang et al., 2021a), has been widely used to manipulate light absorption for enhancing photocatalytic activity. Some plasmonic noble metals (such as Au and Ag) have been successfully used in photocatalysis under Vis-light and NIR-light irradiation through morphology, size and component control, for maximizing the utilization of full spectrum solar energy in wastewater treatment (Chen et al., 2013a; Liang et al., 2020; Vaiano et al., 2019; Wu et al., 2013; Zhao et al., 2019).

Table 1
The performance comparison of pollutants degradation over noble metals-based nanocomposites according to their disparate role in photocatalytic oxidation.

Role	Noble metals	Nanocomposites	Size of noble metals (nm)	Pollutants	Efficiency (rate constant)	Manifestation of noble metals	Ref.
Light harvesting units	Au	TiO_2 NBs[a]/Au NPs	5–15	Tetrabromobisphenol A	97% degradation within 100 min ($0.0317\ min^{-1}$)	The visible light response was enlarged over 570 nm.	(Chen et al., 2014b)
		Au@CNT[b]@TiO_2	11–16	Methylene orange	97% degradation within 60 min ($0.0158\ min^{-1}$)	The overall light absorption was enhanced.	(Misra et al., 2020)
		BTO[c]-Au NRs	51	a-naphthol Rhodamine B	98% degradation within 60 min ($0.0307\ min^{-1}$) 100% degradation within 20 min ($0.2566\ min^{-1}$)	The optical adsorption range was enlarged to 400–1400 nm.	(Li et al., 2018a)
	Ag	Ag@P25[d]	1–3	Rhodamine B	100% degradation within 30 min ($0.1130\ min^{-1}$)	The optical adsorption range was 400–800 nm.	(Chen et al., 2013a)
		Ag/WO_3-110	~4	Methylene orange	98% degradation within 200 min	The optical adsorption range was significantly enhanced in the visible region.	(Ding et al., 2017)
		Ag/$AgGaO_2$	–	Methyl blue	95% degradation within 180 min	The visible-light absorption was in the range of 420–700 nm.	(Zhang et al., 2017)
Electron sinks/ bridge	Au	$BaTiO_3$/Au/g-C_3N_4	–	Rhodamine B	100% degradation within 20 min	Au NPs served as electron mediator between $BaTiO_3$ and g-C_3N_4.	(Wu et al., 2020)
		$BiVO_4$-Au@CdS		Rhodamine B	96% degradation within 180 min ($0.0430\ min^{-1}$)	Au NPs received the photogenerated electrons from $BiVO_4$ and holes from CdS.	(Ye et al., 2018)
	Ag	Ag/mpg-C_3N_4[e]	Ag single atom	Bisphenol A	98% degradation within 60 min	A Schottky barrier was formed thus promoting the separation of charge carriers.	(Zhu et al., 2017)
		WO_3/Ag/CN[f]	–	Rhodamine B Tetracycline	96.2% degradation within 40 min ($0.0530\ min^{-1}$) 90% degradation within 140 min ($0.0150\ min^{-1}$)	Ag NPs could receive the photogenerated electrons from WO_3 and holes from CN.	(Chen et al., 2019b)
	Pt	SnO_2/Pt/In_2O_3	–	2,4-dichlorophenol	90% degradation within 180 min ($0.0237\ min^{-1}$)	Pt served as electron bridge, in which the photogenerated electrons from SnO_2 transferred to Pt through the Schottky barrier and then recombined with holes from In_2O_3.	(Sun et al., 2020b)
		BiOI/Pt/g-C_3N_4	–	Phenol Tetracycline hydrochloride	71.2% degradation within 180 min ($0.0077\ min^{-1}$) 83.1% degradation within 180 min ($0.0514\ min^{-1}$)	Pt acted as a channel for the combination of photogenerated electrons from BiOI and holes from g-C_3N_4.	(Jiang et al., 2020)
Catalytic active sites	Pt	Pt-porous TiO_2	Pt single atom	Toluene	58.95% removal rate within 0.6 s residence time	Electrons on Pt single atom could effectively react with O_3 thus producing $O_3^{\bullet-}$ and $O_2^{\bullet-}$ and degrading toluene.	(Xu et al., 2020)
		Pt/MO[g]	3–4	Toluene	90% removal rate	Pt NPs provided more active sites for toluene oxidation.	(Yu et al., 2020a)

[a] NBs, nanobelts.
[b] CNT, carbon nanotubes.
[c] BTO, bismuth titanate nanosheets.
[d] P25, commercial TiO_2.
[e] mpg-C_3N_4, mesoporous g-C_3N_4.
[f] CN, g-C_3N_4.
[g] MO, octahedral manganese oxide.

2.1.1. Morphology control

As to plasmonic Au-based photocatalysts, there are diverse morphology structures of Au such as nanorods, nanosphere, and nanostar, and nanocages. (Gołąbiewska et al., 2016; Yen et al., 2009; Zhao et al., 2015), which exhibit different response ability towards light region. Among the various morphology of Au, Au nanorods (Au NRs) and Au nanocages (Au NCs) possesses longitudinal plasmonic absorption, in addition to the transverse plasmonic absorption (at 520–540 nm) that is similar to Au NPs. The longitudinal plasmonic absorption along the axial direction is largely determined by aspect ratio of Au NRs and Au NCs (Jiang et al., 2016; Li et al., 2014; Wang and Astruc, 2015). With the aspect ratio of Au NRs and Au NCs increasing, it could proper broaden the light utilization including the full range of Vis-light and part of NIR regions, and thus help synthesize photocatalysts with maneuverable light absorption ability (Chen et al., 2013b; Huang et al., 2006; Li et al., 2018a). Generally, it is hard to compare the improvement effect of noble metals with different morphologies in different study. But in a study from Golabiewska et al., the photocatalytic degradation for phenol by TiO_2 modified with different morphologies of Au, such as nanospheres, nanostars, and nanorods, was conducted to further study the effect of

morphology (Gołąbiewska et al., 2016). The photocatalytic activity in Vis-light region of noble metals with different morphologies decreased in the following order: nanospheres > nanorods > nanostars.

2.1.2. Size control

It can be easily known that plasmonic noble metals-based photocatalytic activity could be promoted when LSPR absorption is enhanced. The size of noble metals would significantly affect the LSPR absorption ability. To explore the correlation, some attention has been focused on studying the size effect of LSPR during photocatalytic degradation (Bai et al., 2016; Mittal et al., 2018; Rani et al., 2021). Generally, the smaller NPs at a certain loading amount was beneficial for promoting the SPR effect, leading to more visible light harvesting and thus enhancing the catalytic activity (Ding et al., 2017; Jiang et al., 2014; Kamarudin et al., 2021; Li et al., 2018b). For example, the Ag-1%@P25 with diameter of 1–3 nm displayed the best photocatalytic activity for RhB degradation, which was 22-fold higher than commercial P25 and~6 times than Ag-0.5%@P25, Ag-5%@P25 and Ag-10%@P25 (Fig. 1a) (Chen et al., 2013a).

But for other groups, they reported other phenomenon of size effect on LSPR absorption ability of noble metals (Trabelsi et al., 2017). That is, the proper increase of noble metals size would be beneficial for enhancing catalytic activity, which is related to localized electric field of LSPR. When the size of noble metals increases, the localized electric field may be enhanced, thus exciting the semiconductors and finally promoting the photo-reaction. Taken the Ag-α-Fe_2O_3 nanocomposite as example, the LSPR peak exhibited a slight red-shifted and the peak becomes broader with Ag size increasing (Zhang et al., 2014). And the photocatalytic activity of the nanocomposites for RhB degradation was gradually improved with the increase of Ag NPs size, and then decreased when the size was over 13.6 nm. Similar results were also found in M@SiO_2 (M = Au, Ag) composites synthesized by Lee et al (Lee et al., 2017). Overall, the size of noble metals significantly affects the LSPR, thus influencing the catalytic activity, but there is no consensus on how the size of noble metal affect. To better get insight, more focus could be paid to figure out the size effect when keeping other condition the same, such as loading amount, morphology of noble metals.

2.1.3. Component control

The LSPR effect is strongly influenced by different noble metals component (Xie et al., 2018). Generally, the plasmon absorption band of Ag NPs is located at 380–420 nm and Au NPs is located at around 520 nm (Jin et al., 2016). As for single component of noble metals, Au NPs are more available because the resonant wavelength of Au NPs locates at the Vis-light region, and are more chemically stable and resistant (Ding et al., 2017; Ju et al., 2020; Wang and Astruc, 2014). In actual application, the component and morphology of different noble metals can be adjusted to complement each other, so as to achieve the maximum utilization of solar light (Bai et al., 2015; Chen et al., 2017; Mittal et al., 2018; Osajima et al., 2021). Overall, the integration of plasmonic noble metals with semiconductors could broaden light absorption range from UV-Vis-NIR regions owing to the LSPR effect, which can be adjusted by tailoring the size, shape or component of plasmonic noble metals.

2.2. Co-catalyst as electron sinks/bridge

Promoting photogenerated charges separation is an effective strategy

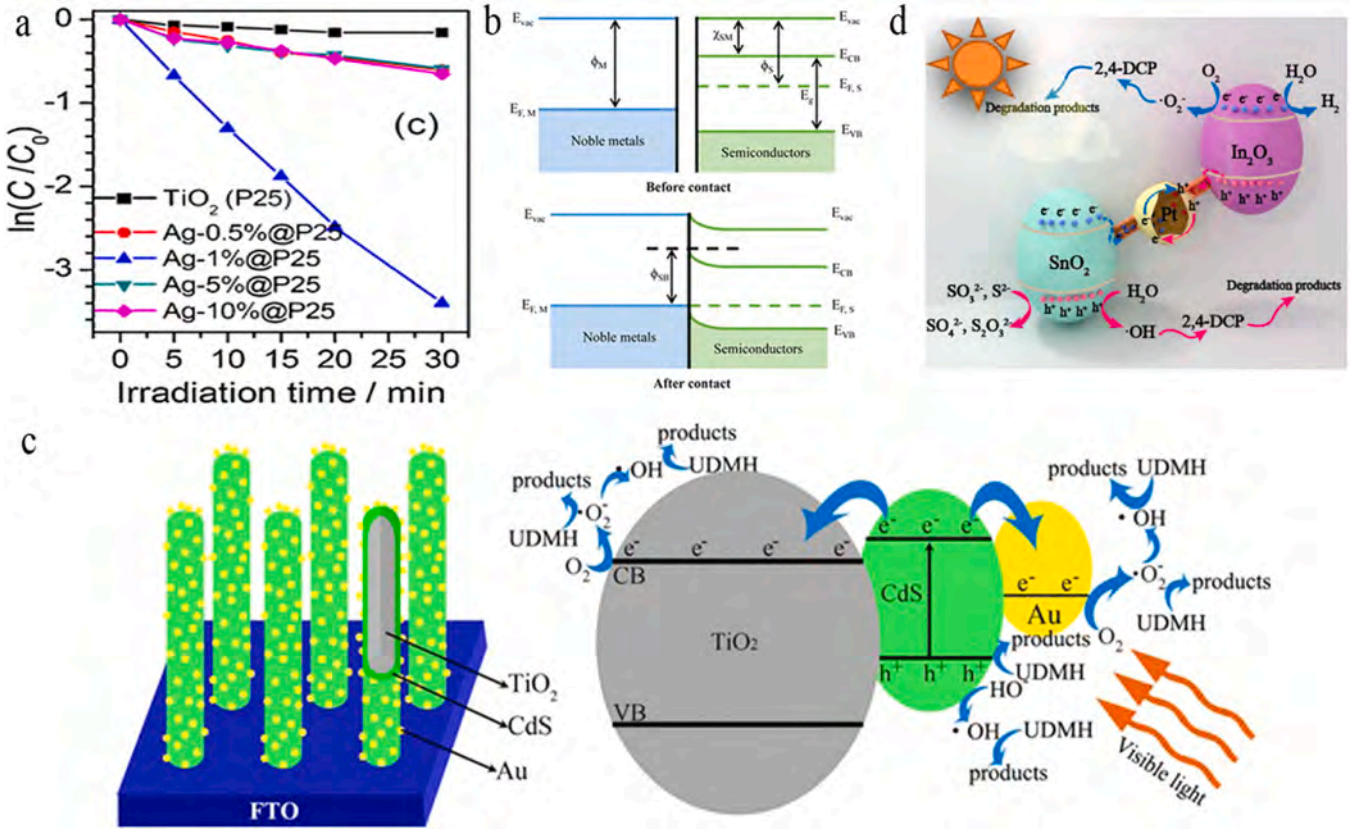

Fig. 1. (a) Plots of $\ln(C_t/C_0)$ vs. reaction time for photodegradation of RhB over P25 and Ag@P25 with various Ag content under Vis-light irradiation. (b) Band structure for noble metals and semiconductors before contact/after contact. (c) Mechanism of UDMH photocatalytic degradation over TiO_2 NRAs/CdS/Au under Vis-light irradiation. (d) Mechanism of 2,4-DCP degradation over SnO_2/Pt/In_2O_3 under Vis-light irradiation.
(a) Reproduced with permission from Chen et al. (2013a) Copyright 2013 Elsevier. (b-c) Reproduced with permission from Gao et al. (2017) Copyright 2017 Nature Publishing Group. (d) Reproduced with permission from Sun et al. (2020b) Copyright 2020 Elsevier.

for enhancing photocatalytic efficiency. Among the strategies for promoting photogenerated charges separation, noble metals often used as co-catalyst as electron sinks/bridge in photocatalysts: (i) fabricating Schottky junction with an appropriate semiconductor; (ii) constructing Z-scheme with semiconductors (Wang et al., 2016; Zhong et al., 2021). All the strategies aim at facilitating the separation of photogenerated charges, thus making the photogenerated electrons or holes stay on semiconductors to effectively participate the redox reactions.

2.2.1. Schottky junction

As for Schottky junction, generally, when noble metals are combined with semiconductors, a potential difference is formed at their metal-semiconductor interface owing to their different work functions (Li et al., 2007; Subramanian et al., 2001; Xiong et al., 2010). The potential difference causes the electron transfer to generate Schottky junction, and the band bending is constructed when the Fermi energy reaches equilibrium between metal and semiconductors (Fig. 1b). As for most noble metals/semiconductors photocatalysts, the Schottky junction can induce photogenerated electrons to directly migrate from semiconductor to noble metals via built-in internal electric field (Chen et al., 2019a). It could efficiently prevent that electrons or holes flow back from noble metals to the semiconductor, resulting in a unidirectional flow channel and thus promoting the separation of photogenerated electron-hole pairs (Zhu et al., 2017). The property endows noble metals the electron sink property to promote the photocatalytic degradation of pollutants (Ismail et al., 2009; Peng et al., 2019; Xiong et al., 2010). Similarly, as for ternary photocatalysts, the electron also follows the unidirectional flow channel from semiconductors to noble metals (Fig. 1c) (Gao et al., 2017).

Actually, the ability of noble metals combing with semiconductors to form Schottky junction is largely depended on the work functions (Liu et al., 2017b). Pt is recognized as the most efficient cocatalysts owing to its large work function among the several noble metals (Meng et al., 2019b). The work function of Pt is 5.64 eV versus E_{vacuum} (1.1 eV vs NHE), which is larger than that of most semiconductors (Aiyun et al., 2016). Therefore, the process of electrons transferred from semiconductors to Pt is more easily. In contrast, other metals possess smaller work function, leading to the weakened driving force of electron transfer, which is depended on Fermi level difference between most semiconductors and noble metals. It illustrated that Pt is more effective than other noble metals when it combines with semiconductors for transferring and reserve electrons. Hence, Pt/semiconductors may exhibit superior catalytic efficiency for pollutants degradation. Taken different noble metal NPs (Ag, Pd, and Pt) anchored TiO_2 photocatalysts as example (Li et al., 2016), Pt-TiO_2 photocatalyst for perfluorooctanoic acid (PFOA) degradation was 12.5-fold higher than pure TiO_2, while Pd-TiO_2 and Ag-TiO_2 photocatalysts were only 7.5 and 2.2-fold higher than pure TiO_2, because the electrons could be easily transferred from CB of TiO_2 to Pt.

2.2.2. Noble metal-based Z-scheme system

As for another strategy for promoting photogenerated charges separation, Z-scheme system-based photocatalysts with noble-metal NPs as electron bridges could be constructed (Meng et al., 2019a). Specifically, in a typical Z-scheme photocatalytic system, the photogenerated electrons produced on one semiconductor would transfer and recombine with the photogenerated holes produced by other semiconductor, leaving the photogenerated electrons at a relatively higher position and the photogenerated holes at a lower position, thus could effectively involve in the ROS production reactions (Low et al., 2017). When involving noble metal in the Z-scheme photocatalytic system, Z-scheme photocatalysts with the structure of semiconductor I/noble metal NPs/semiconductor II were often designed (Zhong et al., 2021). Generally, noble metal NPs were placed between two semiconductors to serve as charge "bridge" as shown in Fig. 1d. In detail, noble metal NPs could receive photogenerated electrons from semiconductor I, and photogenerated holes from semiconductor II, which could effectively protect the holes on the VB of semiconductor I and the electrons on the CB of semiconductor II, thus accelerating charge transfer (Wang et al., 2019b; Yu et al., 2020b). So far, various Z-scheme system-photocatalysts with noble metals as electron bridges have been widely developed to photocatalytic pollutants degradation, which display boosted photocatalytic activity, such as Ag-bridged 2D/2D $Bi_5FeTi_3O_{15}$/g-C_3N_4, $SrTiO_3$/Ag/Ag_3PO_4, SnO_2/Pt/In_2O_3, $BaTiO_3$/Au/g-C_3N_4, Cu_2O/Au/-$BiPO_4$ and $BiVO_4$-Au@CdS (Li et al., 2015a; Sun et al., 2020b; Wang et al., 2019b; Wu et al., 2020; Ye et al., 2018; Yu et al., 2020b).

Serving as electron sink or bridge, noble metals can efficiently facilitate the separation of photogenerated charges, which depends on the work function of noble metal and semiconductors, deposition positions of noble metals on the semiconductor, and surrounding environment (Chen et al., 2019a; Li et al., 2018c; Pulido Melián et al., 2012; Zhao et al., 2016). In addition, it is worth noting that noble metals serving as electron sinks can not only facilitate the separation of photogenerated charges and thus promote photocatalytic oxidation reaction, but also function as active sites for photocatalytic reduction of many reducible pollutants such as nitroaromatics and Cr (VI), illustrating the excellent electron sink property of noble metals (Misra et al., 2020; Patnaik et al., 2020; Qiu et al., 2019).

2.3. Co-catalyst as catalytic active sites

In addition, active sites, producing more ROS or activating redox reaction, are also vital for a photocatalyst (Yu et al., 2010). Noble metals could serve as direct catalytic active sites, which could be excited to produce hot electrons as active catalytic sites under resonant excitation, thus performing the catalytic reaction (Lang et al., 2018; Li et al., 2013; Liu et al., 2018a; Zhang et al., 2018d). The activity for noble metals as active sites is also related to the work functions (Sun et al., 2020a; Trang et al., 2020; Yu et al., 2018). The higher work function is conducive reserve electrons, thus could furnish active sites for producing $O_2^{\bullet-}$. In the research of Abdel-Wahab et al., different noble metals (Ag, Au and Pt) anchored on TiO_2 photocatalysts were constructed for photocatalytic degradation of acetaminophen (AP) (Nasr et al., 2019). The enhanced catalytic activity for AP degradation was because noble metals (Ag, Au and Pt) could furnish active sites for producing of •OH and $O_2^{\bullet-}$. Among the noble metals (Ag, Au and Pt) anchored on TiO_2 photocatalysts, Pt/TiO_2 photocatalysts exhibited the highest photocatalytic performance, which was because Pt possessed better activity than Ag and Au. Recently, a number of studies have reported noble metals serving as catalytic sites for photocatalytic degradation of volatile organic compounds (VOCs), which greatly improves the surface active sites of catalyst and increases the contact opportunity with VOCs (Chen et al., 2016; Fu et al., 2019b; Liang et al., 2021; Liu et al., 2019b; Xu et al., 2020; Yu et al., 2020a; Zhang et al., 2019).

3. The roles of noble metals in Fenton/Fenton-like oxidation process

Fenton oxidation as efficient technologies have been widely studied to degrade pollutants via producing highly reactive •OH in the Haber-Weiss cycle (Li et al., 2019b; Yan et al., 2016; Ye et al., 2020; Zhou et al., 2020b), known as chain reactions $\bullet OH + H_2O_2 \rightarrow H_2O + O_2^{\bullet-} + H^+$ and $O_2^{\bullet-} + H^+ + H_2O_2 \rightarrow O_2 + \bullet OH + H_2O$. To overcome the drawbacks of traditional Fenton oxidation such slow redox cycle, accumulated iron sludge and hazardous H_2O_2 transportation, there have been many studies using noble metals-based catalysts to drive Fenton-like related reaction. Under certain circumstances, noble metals can act as both electron donors or electron acceptors, so noble metals-based catalysts can be used as multifunctional catalysts in Fenton-like reactions to efficiently decompose H_2O_2 to produce •OH, increase the metal redox cycle, or produce H_2O_2 in-situ to reduce the risk in transportation and addition of H_2O_2. Table 2 clearly displays the

Table 2
The performance comparison of noble metals-based nanocomposites according to their disparate role in Fenton/Fenton-like oxidation.

Role	Noble metals	Nanocomposites	Size of noble metals (nm)	Pollutants	Efficiency	Manifestation of noble metals	Ref.
As catalyst for producing •OH	Au	Au/HAp[a]	4.9	Phenol	82% conversion at 343 K	A redox process $Au^0 \leftrightarrow Au^{\&+}$ may occur to activate H_2O_2 producing •OH.	(Han et al., 2008)
		Au/HO-npD[b]	<1	Phenol	93% degradation at room temperature	Au played a role in electron relay from oxidation to the reduction semi-reaction and the reduction process would produce •OH.	(Navalon et al., 2010)
		Au/SRAC[c]	4.4	Bisphenol A	89% conversion at 313 K	Au active sites with dangling carbon atoms displayed partially negatively charged or polarized, and the redox process would decompose H_2O_2 producing •OH.	(Yang et al., 2013)
	Ag	Ag/D3[d]	3.2	Phenol	Rate constants = 4.73 s^{-1}	Ag acted as an efficient photo-Fenton active sites for producing •OH.	(Espinosa et al., 2015)
As catalyst for activating atomic hydrogen	Pd	Pd/Al_2O_3	–	Benzoic acid	80.12% degradation with 12he mechanism of Pd-based catalysts for prom0 min	Pd/Al_2O_3 with large surface area was beneficial for producing atomic H*, subsequently promoting Fe^{3+} reduction to Fe^{2+}.	(Zeng et al., 2020)
		Pd/MIL-101(Cr)	6.5	4-chlorophenol	100% degradation with 90 min	Pd^0 could efficiently retain H_2 and thus activated H_2 to produce atomic H* for promoting Fe^{3+} reduction.	(Liu et al., 2019c)
		$Pd@Fe_3O_4$@MOFs	20	2-cholophenol	100% degradation with 120 min	The electron enriched in Pd NPs would transfer to Fe_3O_4, leading to fast regeneration of Fe^{3+}.	(Niu et al., 2018)
				2,4,6-trichlorophenol	75% degradation with 120 min		
				Phenol	100% degradation with 10 min		
As catalyst for generating H_2O_2	Au	$Au@Mn/MoS_2$	Single atom	Methyl blue	H_2O_2 yield: 1.5 mM in 6 h at visible light irradiation; Methyl blue degradation: 100% with 60 min	Au enhanced the H_2O_2 generation ability of MoS_2, owing to the decreased recombination of photogenerated charge carriers.	(Song et al., 2019a)
		Au/ZnO	4–7	–	H_2O_2 yield: 18.3 mM in 12 h at UV light irradiation	Au exhibited high selectivity for 2e- oxygen reduction reaction (ORR), facilitating the H_2O_2 formation.	(Meng et al., 2020)
	Pd	Pd/C[e]	–	Rhodamine B	H_2O_2 yield: 53.1 mg/L in 120 min at pH 2 and a current of 100 mA; Rhodamine B degradation: 100% with 30 min (0.1090 min^{-1})	Pd was beneficial for adsorbing superoxo molecule, and then interacted with a hydrogen atom dissociated by Pd, thus contributing to production of H_2O_2.	(Yuan et al., 2011)
		Pd NP-PTH-CNTs[f]	5.33	Amaranth	Amaranth degradation: 96% with 15 min (0.6 V vs SHE)	Pd with small size displayed high activity in ORR.	(Reyes-Cruzaley et al., 2019)

[a] HAp, hydroxyapatite.
[b] HO-npD, Fenton-treated diamondnanoparticles.
[c] SRAC, Styrene-based activatedcarbon.
[d] D3, Diamond nanoparticlestreated by Fenton and subsequent H_2 annealing reduction.
[e] C, commercial bamboo charcoal.
[f] PTH-CNTs, polythiophen-carbon nanotubes.

performance comparison of noble metals-based nanocomposites according to their disparate role in Fenton/Fenton-like oxidation.

3.1. As Fenton-like catalytic sites for producing •OH

Noble metals could serve as Fenton-like catalysts to effectively catalyze H_2O_2 decompose to produce •OH (Han et al., 2008; Navalon et al., 2010). Among these noble metals, Au NPs are widely used as Fenton-like catalysts to decompose H_2O_2 in the Haber-Weiss cycle (Liu et al., 2020a). Compared with traditional Fenton system, the advantage of Au NPs-based materials as Fenton-like catalysts is the higher standard electrode potential of Au^{n+}/Au ($E^0(Au^{3+}/Au^+) = 1.360$ V vs NHE; $E^0(Au^+/Au^0) = 1.830$ V vs NHE) than Fe^{3+}/Fe^{2+} ($E^0(Fe^{3+}/Fe^{2+}) =$ 0.771 V vs NHE) (Conte et al., 2008; Zhou et al., 2021). The high oxidation state of Au^{n+} with the strong ability to obtain electrons is beneficial to the regeneration of Au^0 in the subsequent reduction reaction. At the same time, the leaching and shedding of Au NPs can be avoided due to the inertness of Au NPs in the natural environment, thereby ensuring the stability of the catalyst. Most importantly, Au NPs-based materials as an iron-free Fenton-like catalyst can avoid the yield of precipitated sludge. The first novel work is Au NPs anchored on hydroxyapatite (Au/HAp) for phenol degradation in Fenton-like reaction (Fig. 2a) (Han et al., 2008). They preliminarily proposed that a redox process Au^{n+}/Au^0 occurred, leading to the production of •OH (Eqs. (1) and (2)) (Suh et al., 2000). The detailed mechanism involves a transformation of positive and neutral states of Au NPs (Fig. 2b) (Mantzavinos and Poulios, 2010; Martín et al., 2011; Navalon et al., 2010).

$$Au^0 + H_2O_2 \rightarrow Au^+ + OH^- + \bullet OH \quad (1)$$

$$Au^+ + H_2O_2 \rightarrow Au^0 + \bullet OOH + H^+ \quad (2)$$

Normally, the size effect of noble metals has a certain impact on the catalytic activity, and the effect on Fenton reaction is no exception (Kiyonaga et al., 2009; Qin et al., 2019b). Most of previous studies have reported that the catalytic activity of noble metals NPs-based catalysts increased with NPs size decreasing, because smaller Au NPs could

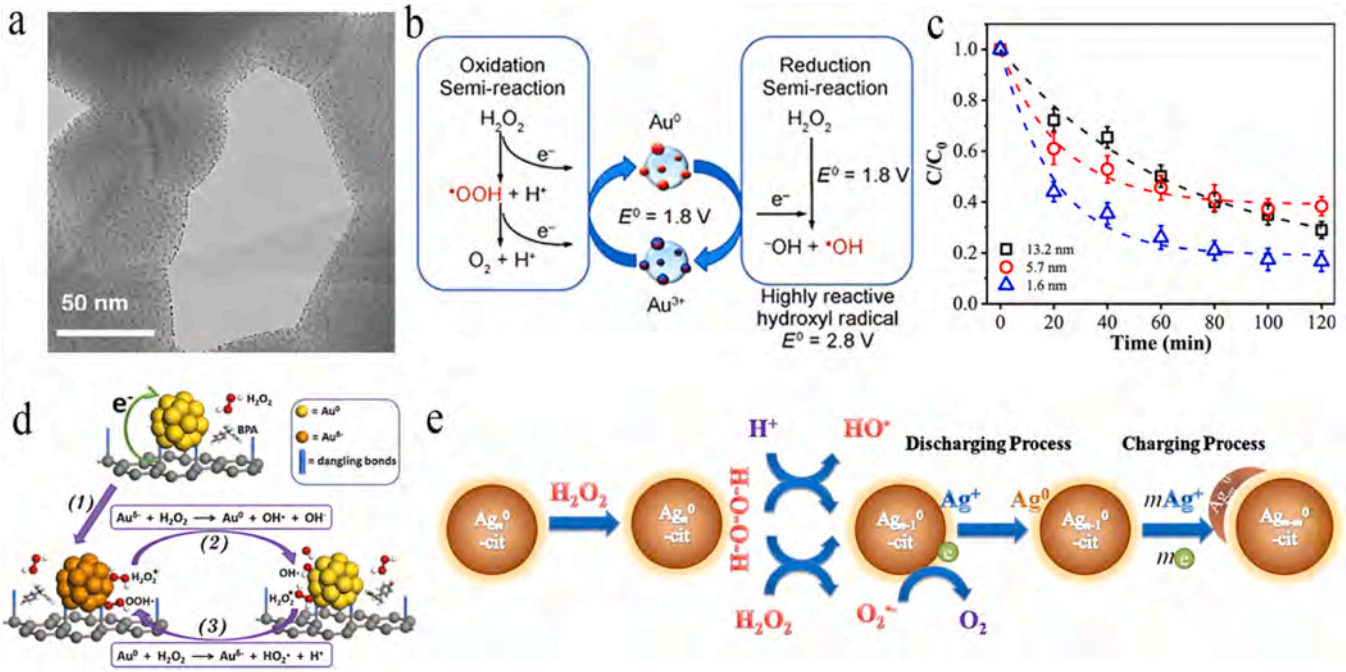

Fig. 2. (a) TEM images of Au/HAp catalysts. (b) Proposed mechanism for phenol degradation in the presence of Au/OH-npD and H_2O_2. (c) TC degradation over Au NCs/CNT with different Au size on TC degradation. (d) The proposed mechanism for •OH production in the Au-Fenton system. (e) The proposed mechanism of H_2O_2 decomposition over Ag NPs/H_2O_2 catalytic system.
(a) Reproduced with permission from Han et al. (2008) Copyright 2008 American Chemical Society. (b) Reproduced with permission from Navalon et al. (2010) Copyright 2010 John Wiley and Sons Ltd. (c) From Liu et al. (2020a) Copyright 2020 American Chemical Society. (d) Reproduced with permission from Yang et al. (2013) Copyright 2013 Elsevier. (e) Reproduced withpermission from He et al. (2014) Copyright 2014 Elsevier.

effectively decompose H_2O_2 to form •OH (Quintanilla et al., 2012). Especially, when the size of Au is less than 2 nm, known as Au nanoclusters (Au NCs), it exhibits highly unique physicochemical behavior and catalytic activity, which is intermediate between single Au atoms and relatively larger Au NPs, and exhibits higher catalytic activity by exposing Au atoms (Cai et al., 2020; Liu et al., 2020a; Wang et al., 2019c). For example, under the same Au loading amounts, Au NCs/CNT catalysts with ultrasmall-sized Au NCs (<2 nm) showed more efficient catalytic performance for TC degradation than Au NPs/CNT catalysts with larger-sized Au NPs (>2 nm), which was because the Au NCs materials possessed higher atom utilization, selectivity and more exposed active sites (Fig. 2c) (Liu et al., 2020a). In addition to size effect of noble metals, the property of supports for anchoring noble metals, and reaction conditions such as pH, dosage of H_2O_2 and temperature also affect the catalytic efficiency of Au NPs-based catalysts towards H_2O_2 decomposition (Martín et al., 2011; Navalon et al., 2011; Naya et al., 2011; Qin et al., 2019b; Yang et al., 2016).

The mechanism of Au NPs-based catalysts towards H_2O_2 decomposition in Fenton-like reaction has been well proposed. Obviously, the mechanism mainly involves the redox cycling of Au^0/Au^{n+} (Au^+ or Au^{3+}) or $Au^{\delta-}/Au^0$, decomposition of H_2O_2 to form •OH, and following the regeneration of Au active sites (Martín et al., 2011; Sha et al., 2016; Shang and Liu, 2011). That is to say, Au NPs-based catalysts in H_2O_2 decomposition reaction also follow the principle of the Haber-Weiss cycle, similar to the traditional Fenton reaction, as shown in Fig. 2d (Liu et al., 2020a; Yang et al., 2013). It has been reported that the negatively charged or partial polarized Au NPs could promote the adsorption and decomposition of H_2O_2 (Yang et al., 2016). Firstly, Au NPs would be polarized or negative electricity. Then, H_2O_2 was decomposed into •OH at the Au-support interface, which was then released to oxidize pollutants. Last, the active sites $Au^{\delta-}$ were regenerated via metallic Au^0 reduced by H_2O_2. Overall, the valence states of the Au NPs are various during Fenton-like reaction, including $Au^{\delta-}$, Au^0, Au^+, and Au^{3+}, which are related to the property, structure and electrophilicity of the supports, the preparation method of Au NPs, as well as pH, etc. Nevertheless, the reason of how the valence states of Au varying during the Fenton reaction remains uncertainty, which is in need of further research.

In addition to Au NPs, the H_2O_2 decomposition is also demonstrated on Ag NPs (Guo et al., 2008; He et al., 2012; Wang and Balbuena, 2005; Zhang et al., 2012). As for Ag NPs/H_2O_2 catalytic system, a charge-discharge type is presented to investigate H_2O_2 decomposition over Ag NPs (Fig. 2e) (Chen et al., 2008; He et al., 2011, 2014; Jones et al., 2011). As for the persulfate-based oxidation systems, noble metal NPs also exhibit potential as peroxymonosulfate activator (Feng et al., 2017; Wang et al., 2017).

3.2. As catalysts for promoting Fe^{2+}/Fe^{3+} redox

Acceleration of metal redox cycle such as Fe^{2+}/Fe^{3+} is important for promoting Fenton/Fenton-like related reactions. Recently, some studies have utilized noble metals to activate H_2 to form activated atomic hydrogen (-H*), which exhibits satisfying reduction ability and thus accelerates the reduction of metal species such as Fe^{3+} (Chaplin et al., 2012; Das et al., 2019). Actually, among noble metals, Pd with lower energy barrier is the most favorable one in H_2O_2 synthesis, because it has higher adsorption energy to H_2 (Jiang et al., 2017). Thus, it can effectively activate H_2 and thus form Pd-H*, and the dissociation energy of Pd-H* is 21–24 kcal/mol, which is relatively low among other transition metals and conducive for -H* to diffuse from active sites (Liu et al., 2019d). The mechanism of Pd-based catalysts for promoting Fe^{2+}/Fe^{3+} redox follows Eqs. (3) and (4), which was firstly demonstrated by Georgi et al. as shown in Fig. 3a (Georgi et al., 2016). The process mainly involved that H_2 was firstly adsorbed and dissociated into H* on Pd surface, which then diffused and reacted with Fe^{3+}, thus regenerating and forming Fe^{2+} (Jiang et al., 2017; Pozzo and Alfè, 2009; Wu et al., 2019a).

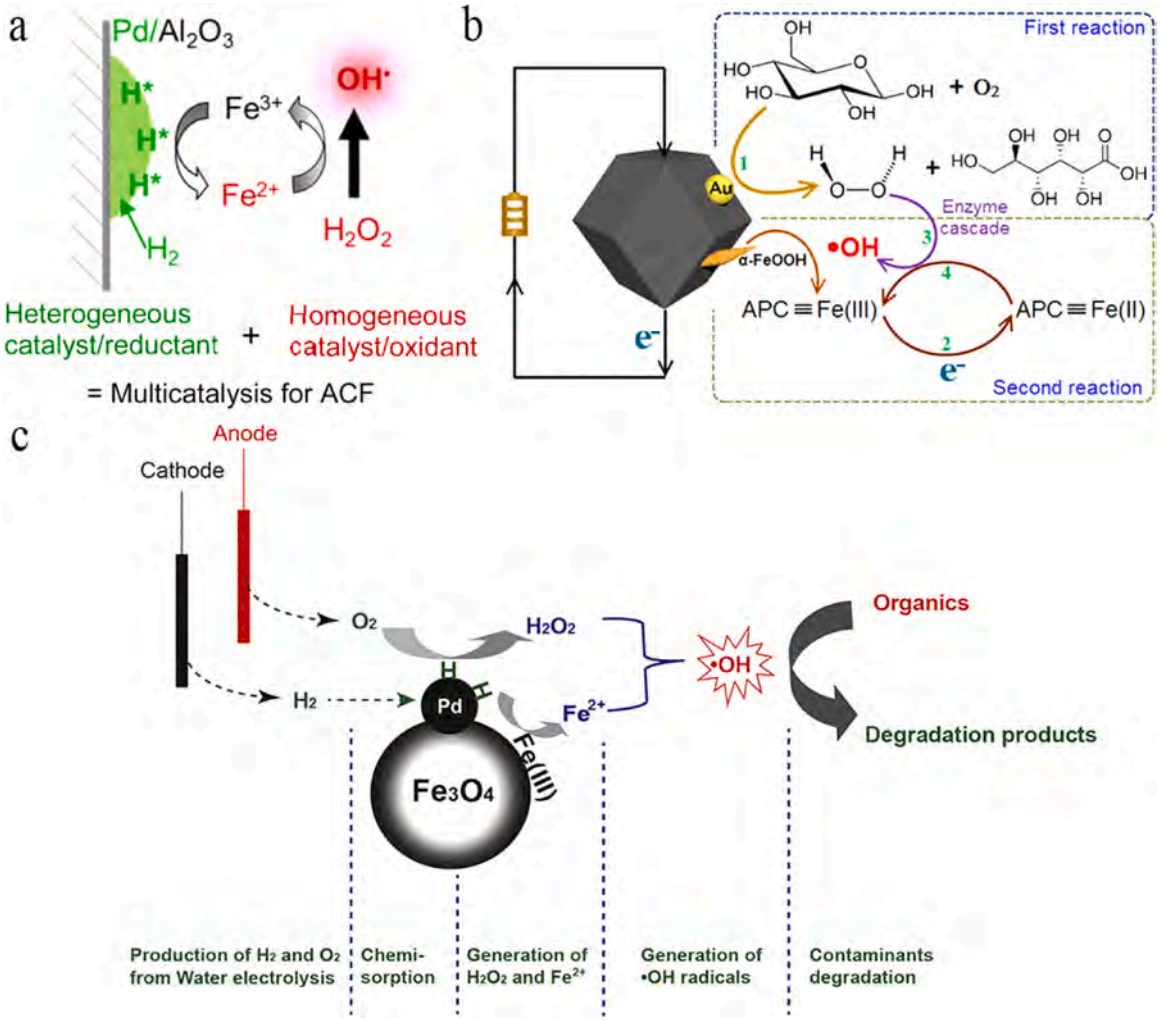

Fig. 3. (a) The proposed mechanism of accelerating Fe^{3+}/Fe^{2+} recycling by -H* produced on Pd/Al_2O_3. (b) Mechanism of H_2O_2 generation over the Au/α-FeOOH–APC catalyst under electro auxiliary. (c) Proposed mechanism of phenol degradation over Pd/MNPs/electro-Fenton system.
(a) Reproduced with permission from Georgi et al. (2016) Copyright 2016 Elsevier. (b) Reproduced with permission from Zhang et al. (2018c) Copyright 2018 American Chemical Society. (c) Reproduced with permission from Luo et al. (2014) Copyright 2014 Elsevier.

$$2 \equiv Pd + \ H_2 \rightarrow 2 \equiv Pd\text{-}H * \quad (3)$$

$$\equiv Pd\text{-}H* \ + Fe^{III} \rightarrow Pd + H^+ + Fe^{II} \quad (4)$$

Additionally, Pd-based electrochemical oxidation systems are researched for acceleration of Fe^{2+}/Fe^{3+} cycling to promote degradation of pollutants (Huang et al., 2017; Qin et al., 2015). In the electrochemical systems, except the reduction of Fe^{3+} by activated -H* on Pd catalysts (Eqs. (3) and (4)), the regeneration of Fe^{2+} can also be ascribed to oxidation dissolution of Fe^{2+} from Fe-compounds by in-situ produced H_2O_2 on noble metal catalysts, or the direct electron transfer from the cathode to reduce Fe^{3+} (Liao et al., 2013; Luo et al., 2014). Some studies have noticed the issue, and found that the -H* on Pd active sites plays the main contribution in the regeneration of Fe^{2+} in Pd-based electrochemical oxidation systems (Luo et al., 2014; Zeng et al., 2020). Pd could provide sufficient active sites for H_2 adsorption and electrical inducing the conversion from H^+ to -H*, thereby accelerating transformation rate of Fe^{3+}/Fe^{2+}. Except -H* over Pd NPs play a role in Fe^{3+} reduction, the Pd were manifested that the electrons enriched on Pd would transfer to Fe species after Fe^{2+} were oxidized by H_2O_2, thus resulting in fast regeneration of Fe^{2+} (He et al., 2019; Li et al., 2015b; Niu et al., 2018).

3.3. As catalysts for generating H_2O_2 in Hydrogen-enabled conditions

In Fenton reaction, establishing H_2O_2-based catalytic reaction concerns the source of H_2O_2, includes the addition and in-situ production of H_2O_2 in reaction system. In-situ production of H_2O_2 can be considered as an ideal method for providing H_2O_2, since O_2 is safe and readily available raw source for H_2O_2 generation (Nogueira et al., 2005; Zhang et al., 2018a). With the assistance of noble metal-based nanocomposites as cathode or catalysts, H_2O_2 can be generated by catalytic hydrogen oxidation or O_2 activation process (Pi et al., 2020). During the synthesis of H_2O_2 generation over noble metal-based nanocomposites, the various hydrogen sources could be effectively utilized by noble metals, such as H_2 gas or hydrogen substitutes (hydrazine, formic acid, and glucose) (Choudhary et al., 2007; Dai et al., 2018; Li et al., 2015b). Recently, an interesting study was reported that Au NPs could catalytically oxidize glucose to synthesize H_2O_2 via a "green" process, similar to the process of natural glucose oxidase (Eq. (5)) (Huang et al., 2020a). Inspired by the characteristics of Au NPs catalytic reaction, the glucose could be used as hydrogen source for H_2O_2 generation in pollutant removal over Au NPs-based catalysts and the mechanism for H_2O_2 generation was displayed in Fig. 3b (Zhang et al., 2018c).

$$\text{Glucose} + O_2 + H_2O \xrightarrow{\text{Au NPs}} \text{gluconic acid} + H_2O \quad (5)$$

Among noble metals, Au and Pd are reported to possess high selectivity and activity for H_2O_2 generation (Cho et al., 2020; Shen et al., 2019b; Song et al., 2020b, 2019a; Zhang et al., 2018b). In some studies, AuPd bimetallic materials are often used for in-situ synthesis of H_2O_2 and achieve efficient degradation of pollutants via electro-Fenton process (Qin et al., 2015; Sun et al., 2015), because Au could affect AuPd nanocrystals and thus provide more exposed -H* that was chemisorbed on the Pd surface, which was beneficial for the H_2O_2 synthesis. However, with Au NPs size increasing to 30 nm, only H_2O instead of H_2O_2 was produced, indicating the practical limitation of Au based catalyst. Hence, in practical, Pd NPs or Pd-based nanocatalysts are usually used for H_2O_2 generation (Liao et al., 2015, 2018; Pi et al., 2020; Xie et al., 2015; Yu et al., 2015). There are a number of studies synthesized H_2O_2 over Pd-based nanocomposites using in-situ electro-generated H_2 and O_2 (Eqs. (6)–(8)) (Liu et al., 2018c; Luo et al., 2014; Tan et al., 2020; Yuan et al., 2011). As shown in Fig. 3c, H_2 and O_2 gas were firstly produced by electrolysis of H_2O, then two H atoms were diffused and chemisorbed onto the Pd surface to react with O_2, resulting in generation of H_2O_2. Under the electro-assistance condition, the applied current intensity or voltage value have considerable impact on the H_2O_2 generation at the cathode. The higher applied current intensity or voltage value is conducive for exposing more activated atoms of noble metals-based materials at cathode. But the generation dosage of H_2O_2 would not always increase with applied current intensity increasing, which is owing to some parasitic reactions (Yan et al., 2016).

$$\text{Anode:} 2H_2O_2 - 4e^- \rightarrow 4H^+ + O_2(g) \quad (6)$$

$$\text{Cathode:} 4H_2O_2 + 4e^- \rightarrow 4OH^- + 2H_2(g) \quad (7)$$

$$H_{2(g)} + O_{2(g)} \xrightarrow{Pd} H_2O_2 \quad (8)$$

In conclusion, small diameter (less than 5 nm) and lack of crystalline order of noble metals should be required for achieving high H_2O_2 selectivity (S. Zhu and Chen, 2020; W. Zhu and Chen, 2020). The superiority of noble metals in H_2O_2 generation primarily depends on the strong binding ability towards O_2, and the ability could be easily adjusted through the metal d electrons and coordination configurations of the active sites.

4. Important characterization technologies for evaluating noble metals

4.1. Emerging characterization techniques

In recent years, some advanced and specific techniques have been used to explore and analyze the working mechanisms of noble metals at atomic-scale level, as well as the relationship between the structures and performance. For example, some advanced characterization techniques such as aberration-corrected scanning transmission electron microscopy (AC-STEM), X-ray absorption spectroscopy (XAS), as well as in-situ characterization techniques such as in situ environmental TEM (ETEM), in situ Fourier transform infrared spectroscopy (FTIR) and in situ XAS, have been used to deeply study the features of noble metal-based catalysts and will be concluded in detail.

4.1.1. AC-STEM and XAS

Different from conventional TEM technique, AC-STEM is developed to identify the atomic-scale active sites of noble metals due to the additive beam current and resolution (Dong et al., 2020). Especially, aberration-corrected high-angle annular dark field scanning transmission electron microscopy (AC-HAADF-STEM) could offer high resolution images at atomic scale through gathering the electrons scattered from a loop near the beam by a loop dark field detector (Wang et al., 2019a). As for noble metals, especially single atoms of noble metals, it could be directly observed from the light spots (even at atomic-scale). For example, the single Pd atoms uniformly located on g-C_3N_4 modified with carbon vacancies (Cv-CN) could be clearly observed from AC-HAADF-STEM as shown in Fig. 4a, with significant contrast. And no Pd sub-nanometer clusters nor nanoparticles could be visualized, further demonstrating the successful synthesis of single Pd atoms (Liu et al., 2021).

Before the appearance of AC-STEM, the fine structural information on noble metals-based nanocomposites mainly depends on the XAS analysis, which is composed of two consecutive regions: the X-ray absorption near edge structure (XANES) and the extended X-ray absorption fine structure (EXAFS) (Zhang et al., 2021c). The former could offer information about the valence state and coordination geometry of noble metals with supported materials. And the latter could reflect the many local structural information about the absorbing atoms (Dong et al., 2020). XAS cannot provide visualized evidences as those from electron microscopy, but it is more informative for multiple-shell/component analysis. Usually, XAS analysis equipped with other characterization technique such as STEM, XPS and nuclear magnetic resonance (NMR) spectroscopy is used to better understand the noble metals-based nanocomposites at atomic scale (including single atoms of noble metals catalyst) (Nan et al., 2017).

4.1.2. In-situ characterization techniques

In addition to above ex situ characterization techniques, in situ/operando characterization techniques for noble metals-based nanocomposites characterization have been developed to better identify active sites and monitor the variation of geometric structure and electronic environment.

(i) In situ ETEM: a gas-in-microscopy operation method. It requires confinement of the gas environment near the catalyst at a desired temperature with the high-vacuum electron microscopy column, which can offer more dynamic structure variation under reaction condition. In the study of Corma et al., they found that Pt species could reversibly disintegrated and aggregated under the conditions of 500–550 °C in O_2 (oxidized atmosphere) and 300–400 °C in H_2 (reductive atmosphere) under in situ ETEM (Liu et al., 2018b), indicating that the structure of Pt species encapsulated on MCM-22 was super sensitive to the gas reactants and temperature.

(ii) In situ XAS: sensitivity analysis of local structure and valence state with a quick scanning rate (approaching picoseconds) under various chemical conditions (Chen et al., 2014a). Commonly, the analysis of the absorption spectra is based on comparing the tested spectra with some known structural properties that have been manifested (Yuan et al., 2019). In the system of Ag@FAU systems, in situ Ag-K edge XANES spectra were recorded as temperatures increasing. The energy changes of pretreated samples obviously displayed that the oxidation states of Ag cluster in FAU zeolite altered (Yamamoto et al., 2009).

(iii) In situ FTIR: the common used modes include in situ transmission IR (TIR), diffuse-reflectance IR Fourier Transform (DRIFT), attenuated total reflection IR (ATR-IR), and reflection-absorption IR (RAIR) similar to the ex situ FT-IR method. Generally, CO-probed FTIR analysis was often used for identifying the site of noble metal single atoms-based catalysts, and ratio of different metals in the multiple metallic catalysts (Dong et al., 2020; Tou et al., 2019).

Usually, multiple in situ characterization techniques are simultaneously conducted to get better insight into the noble metal-based catalysts at the atomic level (Godoi et al., 2016). Although the recent progress on the advanced characterization techniques such as in situ methods provides more information for identifying the instinct properties and mechanism, the further understanding and utilization of in situ characterization techniques should be focused, and more challenges are

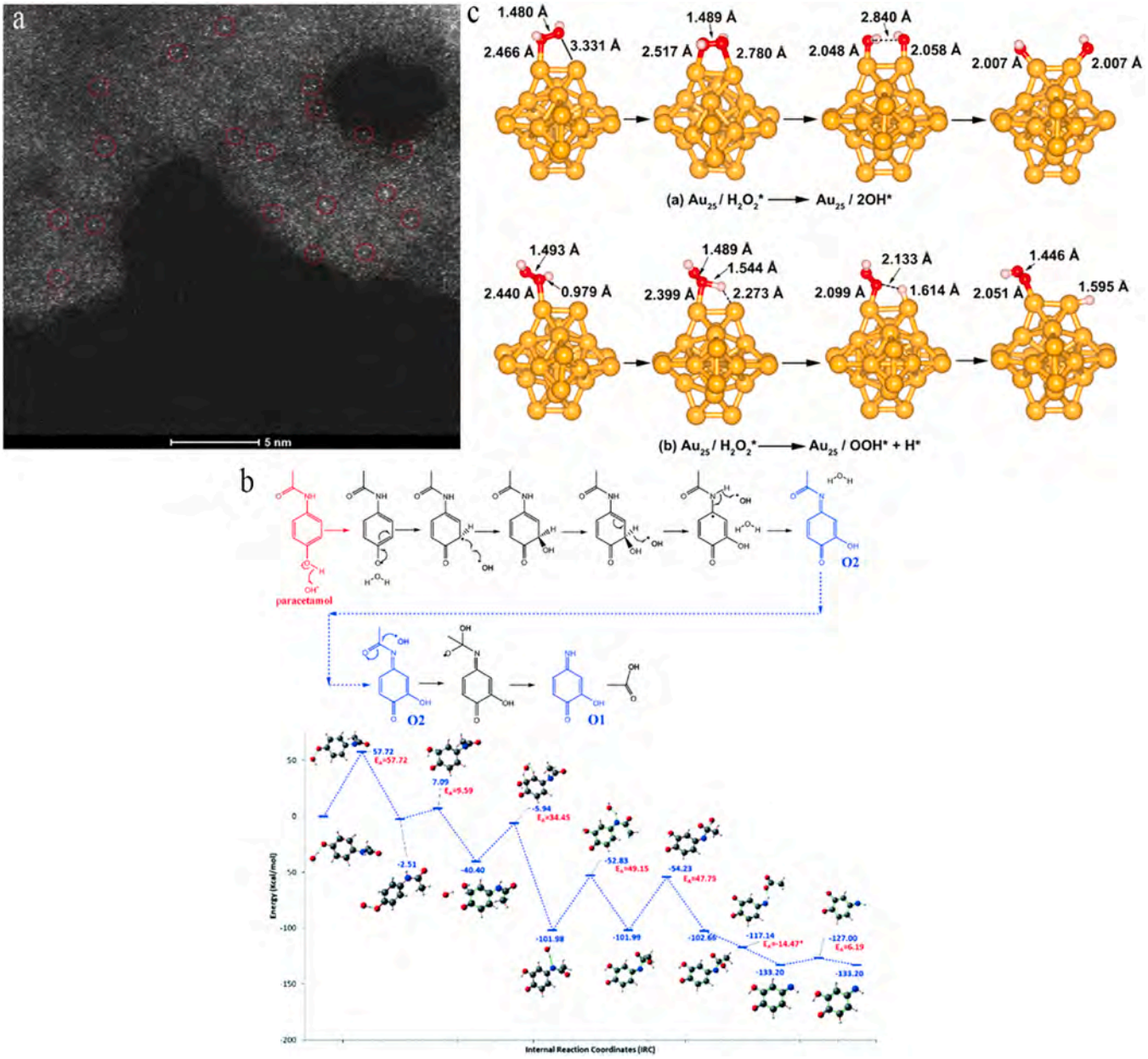

Fig. 4. (a) AC-HAADF-STEM of Pd atoms anchored g-C_3N_4. (b) Degradation pathway of paracetamol catalyzed by $ZnFe_2O_4$-Au. (c) Proposed routes (1 and 2) of H_2O_2 decomposition over AuNCs/CNT surface.
(a) Reproduced with permission from Liu et al. (2021) Copyright 2021 Elsevier. (b) Reproduced with permission from Huerta-Aguilar et al. (2019) Copyright 2019 Royal Society of Chemistry. (c) Reproduced with permission from Liu et al. (2020a) Copyright 2020 American Chemical Society.

proposed in the perspective.

4.2. Theoretical calculation

Generally, theoretical calculations can provide structure information at atomic scale of noble metals-based nanocomposites such as electronic structure, supply the activation energy barriers of reaction and verify the function of each structure (Deng et al., 2020; Fu et al., 2019a; Hu et al., 2012; Ma et al., 2017; Zhang et al., 2021b), which can supplement the experimental results. Density functional theory (DFT) calculations are often performed to reveal the properties of noble metals-based photocatalysts, such as the electronic band structures, Hirshfeld charge, and DOS, and highest occupied molecular orbital-lowest unoccupied molecular orbital (HOMO-LUMO) transition could be obtained (Ma et al., 2017; Song et al., 2019b; Tong et al., 2018; Xu and Carter, 2019; Yang et al., 2020b, 2020d; Zhao et al., 2018). Except for basic properties analysis for noble metals-based catalysts, DFT calculation could be also performed for better understanding the catalytic degradation mechanism, which is most important for analyzing degradation products. A number of studies have used DFT analysis based on Gaussian or Vienna Ab initio Simulation Package (VASP) to research the reaction mechanism. Taking Au-based catalysts in catalytic pollutants degradation as examples, DFT analysis has been performed to deeply study the characteristic of catalysts and catalytic mechanism in oxidation process (Huerta-Aguilar et al., 2019; Liu et al., 2020a). As shown in Fig. 4b, DFT analysis demonstrated that •OH produced on $ZnFe_2O_4$-Au system firstly attacked paracetamol and thus formed several possible intermediates via a high energy transition state. And the total energy differences gradually reduced in each step until the final product was produced, indicating oxidation rate of paracetamol was slow at initial period and

then accelerated with reaction rate getting higher. In addition, it was reported that DFT analysis based on VASP was performed to study the production, adsorption, and decomposition paths of H_2O_2 over Au NPs/CNT catalysts in Fenton-like reaction (Fig. 4c).

5. Conclusions and perspectives

This review innovatively classifies the roles of noble metals according to their disparate functions in photocatalytic oxidation and Fenton/Fenton-like oxidation reactions, and summarizes advanced characterization techniques for evaluating noble metals. In the photocatalytic degradation, noble metals play important roles in enhancing light harvesting, facilitating photogenerated charge carrier separation/transfer, and providing catalytic active sites. The roles of noble metals in Fenton/Fenton-like systems mainly include: as active sites for decomposing H_2O_2 to produce •OH, accelerating Fe^{2+}/Fe^{3+} redox and in-situ producing H_2O_2. Overall, integrating the multifunctional noble metals with other nanomaterials (supports or semiconductors) can improve the catalytic activity in the oxidation degradation of pollutants and noble metals play important roles in boosting performance of nanocomposites.

Despite noble metals-based catalysts make some progress in the component and structure design and have certain potential in solving environmental issues, many challenges still remain to design and synthesize nanocomposites, which needs to solve for fully exerting the capabilities of noble metals.

(1) Continuing exploring the fundamental understanding of catalytic mechanism over noble metals-based nanocomposites by in situ/operando characterization techniques is urgently needed for dynamic monitoring the process under working conditions. Dynamic monitoring the reaction of noble metals-based nanocomposites during photocatalytic oxidation and Fenton/Fenton-like oxidation is conducive to analyze the domination mechanism and variation in the geometric or electronic structure, thus analyzing different reaction pathways. It could find the vital impact on an enhanced catalytic activity by analyzing dynamic structural variation of the interaction between noble metals and other nanocomposites. At present, a majority of studies have performed in situ/operando structural characterizations at gas phase reaction conditions. However, most applications of noble metals-based nanocomposites in photocatalytic oxidation and Fenton/Fenton-like oxidation for organic pollutants degradation are under liquid phase reaction conditions. Hence, the in situ/operando structural characterizations should be further upgraded through integrating more techniques to achieve dynamic monitor for complex liquid reactions.

(2) Expect in situ/operando characterization techniques, further fundamental understanding of catalytic mechanism over noble metals-based nanocomposites should be analyzed by theoretical calculations. Exactly, the insight on the mechanism could be obtained through combing theoretical calculations with experimental measurements. It could reasonably account for the experimental results for revealing the photocatalytic oxidation and Fenton/Fenton-like oxidation process, and the condition for theoretical calculations should be similar to experimental conditions. The theoretical calculations based on experimental results are helpful and reliable for designing a novel efficient noble metals-based nanocomposite, and can imitate the available structure of active sites, interaction between noble metals and support surface, and reaction intermediates, and active radicals, as well as the reaction mechanisms. Certainly, the satisfying simulated results acquired by theoretical calculations should be based on the premise of setting well calculated parameters. Then combining with experiment measurements, a more distinct comprehension of the catalytic mechanism over noble metals-based nanocomposites could be obtained. Taking full advantage of theoretical calculations would be better for design a novel and effective noble metals-based nanocomposites with appropriate function in catalytic oxidation for pollutants removal.

(3) How to decrease the cost/usage of noble metals in the nanocomposites should also be concerned, owing to the high cost and scarcity of noble metals. On the one hand, rational utilization the controllable size and morphology property of noble metals is a direct strategy. Specifically, as for noble metals-based photocatalysts, the morphology of plasmonic noble metals could be adjusted to absorb the different light region from Vis-light to NIF region, thus avoiding the addition of other nanomaterials. Taking Au NRs for instance, by regulating the aspect ratio of Au NRs, the absorption spectrum can be adjusted from Vis-light to NIF region. In addition, decreasing the size of noble metals to ultra-small size is a great option to decrease the cost and simultaneously keep the high activity. Preparing noble metal single atoms-based nanocomposites may solve the problems in cost and resource. Actually, there are some studies that reported noble metal single atoms-based nanocomposites exhibit inspired activity in catalytic oxidation for degrading recalcitrant contaminants. But the harsh synthesis conditions may limit their production. Hence, more attention could be focused on the development of controllable technologies to fabricate cost-effective noble metal single atoms-based nanocomposites.

(4) Continuing probing and developing relevant functional noble metals-based nanocomposites is a key issue for realizing superior performance in catalytic oxidation for pollutant removal. As concluded above, when noble metals-based nanocomposites are applied in catalytic oxidation reactions, it usually plays multifunctional properties in the enhancement effect, rather than display only one function, which lies on the property (size and morphology) of noble metals and supports, deposition positions of noble metals on supports/semiconductors (synthesis method), as well as work function of noble metals and semiconductors. Although noble metals-based nanocomposites exhibit multifunctional catalytic ability towards different reaction, some active center of noble metals is not favorable for some reaction pathways. For example, some noble metal single atoms-based nanocomposites is not conducive for electrocatalytic oxidation of small organic pollutants, and breakage of O═O bonds of O_2, impeding the synthesis of H_2O_2. Hence, according to the different requirements on pollutants removal, designing a specific noble metals-based nanocomposite is more beneficial to achieve super high removal efficiency. Overall, the reaction selectivity of noble metals-based nanocomposites still needs to promote by regulating the electronic structure and coordination between noble metals and supports, and during the process, theoretical calculations could be applied, which could verify rationality and reveal the mechanism.

(5) Again, further exploring novel noble metals-based nanocomposites strategies and synthesis means to realize quick and extensive fabrication is promising but challenging for practical applications all the time. For noble metals nanoparticles and nanoclusters, the synthesis methods are diverse and relatively mature, but for noble metals single-atom based catalysts, the synthesis is not enough. Although the novel synthetic method such as atomic layer deposition (ALD) is developing, the synthetic mechanism is still unrevealed and how to realize high metal coverage is needed to achieve. In addition, from a perspective of applications, during synthesis of noble metals-based photocatalysts, the process of decorating noble metals on semiconductors is a bit difficult. It should be noticed that noble metals with small size need to be precisely prepared and controlled to decorate on the desired sites of semiconductors, and the noble metals with relatively high work function may reduce their own benefit when combined with semiconductors. Therefore, the

exploration of noble metals-based photocatalysts should be focused on not only the preparation approach of noble metals, but also the decoration tactics of noble metals on semiconductors.

Declaration of Competing Interest

The authors declare that they have no known competing financial interests or personal relationships that could have appeared to influence the work reported in this paper.

Acknowledgments

This study was financially supported by the Program for the National Natural Science Foundation of China (U20A20323, 51521006, 51879101, 51579098, 51779090, 51909084, 51709101, 51809090), the National Program for Support of Top–Notch Young Professionals of China (2014), and Hunan Natural Science Foundation (2020JJ3009), Hunan Researcher Award Program (2020RC3025), Hunan Provincial Science and Technology Plan Project (2018SK2041), and the Fundamental Research Funds for the Central Universities (531119200086, 531118010114, 531118040083, 541109060031, 531118010473).

References

Aiyun, Meng, Jun, Zhang, Difa, Xu, Bei, Cheng, Jiaguo, Yu, 2016. Enhanced photocatalytic H2-production activity of anatase TiO2 nanosheet by selectively depositing dual-cocatalysts on 101 and 001 facets. Appl. Catal. B Environ. 198, 286–294.

Ayati, A., Ahmadpour, A., Bamoharram, F.F., Tanhaei, B., Manttari, M., Sillanpaa, M., 2014. A review on catalytic applications of Au/TiO2 nanoparticles in the removal of water pollutant. Chemosphere 107, 163–174.

Bai, S., Jiang, J., Zhang, Q., Xiong, Y., 2015. Steering charge kinetics in photocatalysis: intersection of materials syntheses, characterization techniques and theoretical simulations. Chem. Soc. Rev. 44 (10), 2893–2939.

Bai, Y., Chen, T., Wang, P., Wang, L., Ye, L., Shi, X., Bai, W., 2016. Size-dependent role of gold in g-C3N4/BiOBr/Au system for photocatalytic CO_2 reduction and dye degradation. Sol. Energy Mater. Sol. Cells 157, 406–414.

Bogireddy, N.K.R., Sahare, P., Pal, U., Méndez, S.F.O., Gomez, L.M., Agarwal, V., 2020. Platinum nanoparticle-assembled porous biogenic silica 3D hybrid structures with outstanding 4-nitrophenol degradation performance. Chem. Eng. J. 388, 124237.

Cai, J., Javed, R., Ye, D., Zhao, H., Zhang, J., 2020. Recent progress in noble metal nanocluster and single atom electrocatalysts for the hydrogen evolution reaction. J. Mater. Chem. A 8 (43), 22467–22487.

Chaplin, B.P., Reinhard, M., Schneider, W.F., Schüth, C., Shapley, J.R., Strathmann, T.J., Werth, C.J., 2012. Critical review of Pd-based catalytic treatment of priority contaminants in water. Environ. Sci. Technol. 46 (7), 3655–3670.

Chen, D., Chen, Q., Ge, L., Yin, L., Fan, B., Wang, H., Lu, H., Xu, H., Zhang, R., Shao, G., 2013a. Synthesis and Ag-loading-density-dependent photocatalytic activity of Ag@TiO2 hybrid nanocrystals. Appl. Surf. Sci. 284 (nov.1), 921–929.

Chen, F., Wu, C., Wang, J., François-Xavier, C.P., Wintgens, T., 2019a. Highly efficient Z-scheme structured visible-light photocatalyst constructed by selective doping of Ag@AgBr and Co3O4 separately on {010} and {110} facets of BiVO4: Pre-separation channel and hole-sink effects. Appl. Catal. B: Environ. 250, 31–41.

Chen, H., Shao, L., Li, Q., Wang, J., 2013b. Gold nanorods and their plasmonic properties. Chem. Soc. Rev. 42 (7), 2679–2724.

Chen, H., Cao, S., Yao, J., Jiang, F., 2017. Fabrication of Ag nanowires–CdS–Au photocatalyst and its excellent visible light photocatalytic activity: the role of synergetic electron transfer. J. Taiwan Inst. Chem. Eng. 71, 189–196.

Chen, J., Xiao, X., Wang, Y., Ye, Z., 2019b. Ag nanoparticles decorated WO3/g-C3N4 2D/2D heterostructure with enhanced photocatalytic activity for organic pollutants degradation. Appl. Surf. Sci. 467–468, 1000–1010.

Chen, L., Xiang, W., Wu, H., Ouyang, S., Zhou, B., Zeng, Y., Chen, Y., Kuzyakov, Y., 2019c. Tree species identity surpasses richness in affecting soil microbial richness and community composition in subtropical forests. Soil Biol. Biochem. 130, 113–121.

Chen, L.X., Zhang, X., Shelby, M.L., 2014a. Recent advances on ultrafast X-ray spectroscopy in the chemical sciences. Chem. Sci. 5 (11), 4136–4152.

Chen, Q., Liu, H., Xin, Y., Cheng, X., 2014b. Coupling immobilized TiO2 nanobelts and Au nanoparticles for enhanced photocatalytic and photoelectrocatalytic activity and mechanism insights. Chem. Eng. J. 241, 145–154.

Chen, X., Zhu, H.Y., Zhao, J.C., Zheng, Z.F., Gao, X.P., 2008. Visible-light-driven oxidation of organic contaminants in air with gold nanoparticle catalysts on oxide supports. Angew. Chem. Int. Ed. Engl. 47 (29), 5353–5356.

Chen, X., Chen, D., Li, N., Xu, Q., Li, H., He, J., Lu, J., 2019d. Durable and stable MnMoO4-coated copper mesh for highly efficient oil-in-water emulsion separation and photodegradation of organic contaminants. ACS Appl. Mater. Interfaces 11 (26), 23789–23797.

Chen, Y., Huang, Z., Zhou, M., Hu, P., Du, C., Kong, L., Chen, J., Tang, X., 2016. The active sites of supported silver particle catalysts in formaldehyde oxidation. Chem. Commun. 52 (65), 9996–9999.

Cheng, Y., Fan, Y., Pei, Y., Qiao, M., 2015. Graphene-supported metal/metal oxide nanohybrids: synthesis and applications in heterogeneous catalysis. Catal. Sci. Technol. 5 (8), 3903–3916.

Cheng, Z., Guan, H., Meng, J., Wang, X., 2020. Dual-functional porous wood filter for simultaneous oil/water separation and organic pollutant removal. ACS Omega 5 (23), 14096–14103.

Cho, Y.-H., Han, G.-H., Han, S.S., Seo, M.-g, Lee, K.-Y., 2020. Effects of varying amounts of Na on Pd/TiO2 for the direct synthesis of H2O2: Identification of the Pd dispersion and catalytic activity enhancement by changing the surface electronic states. Mol. Catal. 484, 110732.

Choudhary, V.R., Jana, P., Samanta, C., 2007. Generation of hydrogen peroxide via the selective reduction of oxygen by hydrazine sulfate over Br-promoted Pd/Al2O3 catalyst in an aqueous medium at ambient conditions. Appl. Catal. A: Gen. 323, 202–209.

Conte, M., Carley, A., Attard, G., Herzing, A., Kiely, C., Hutchings, G., 2008. Hydrochlorination of acetylene using supported bimetallic Au-based catalysts. J. Catal. 257 (1), 190–198.

Dai, S., Wu, X., Zhang, J., Fu, Y., Li, W., 2018. Coenzyme A-regulated Pd nanocatalysts for formic acid-mediated reduction of hexavalent chromium. Chem. Eng. J. 351, 959–966.

Das, R., Sypu, V.S., Paumo, H.K., Bhaumik, M., Maharaj, V., Maity, A., 2019. Silver decorated magnetic nanocomposite (Fe3O4@PPy-MAA/Ag) as highly active catalyst towards reduction of 4-nitrophenol and toxic organic dyes. Appl. Catal. B: Environ. 244, 546–558.

Deng, J., Song, W., Jing, M., Yu, T., Zhao, Z., Xu, C., Liu, J., 2020. A DFT and microkinetic study of HCHO catalytic oxidation mechanism over Pd/Co3O4 catalysts: the effect of metal-oxide interface. Catal. Today 339, 210–219.

Ding, J., Zhang, L., Liu, Q., Dai, W.-L., Guan, G., 2017. Synergistic effects of electronic structure of WO3 nanorods with the dominant {001} exposed facets combined with silver size-dependent on the visible-light photocatalytic activity. Appl. Catal. B: Environ. 203, 335–342.

Dong, C., Li, Y., Cheng, D., Zhang, M., Liu, J., Wang, Y.-G., Xiao, D., Ma, D., 2020. Supported metal clusters: fabrication and application in heterogeneous catalysis. ACS Catal. 10 (19), 11011–11045.

Espinosa, J.C., Navalón, S., Álvaro, M., García, H., 2015. Silver nanoparticles supported on diamond nanoparticles as a highly efficient photocatalyst for the Fenton reaction under natural sunlight irradiation. ChemCatChem 7 (17), 2682–2688.

Feng, Y., Lee, P.-H., Wu, D., Shih, K., 2017. Surface-bound sulfate radical-dominated degradation of 1,4-dioxane by alumina-supported palladium (Pd/Al2O3) catalyzed peroxymonosulfate. Water Res. 120, 12–21.

Fu, C., Liu, C., Li, T., Zhang, X., Wang, F., Yang, J., Jiang, Y., Cui, P., Li, H., 2019a. DFT calculations: a powerful tool for better understanding of electrocatalytic oxygen reduction reactions on Pt-based metallic catalysts. Comput. Mater. Sci. 170, 109202.

Fu, S., Zheng, Y., Zhou, X., Ni, Z., Xia, S., 2019b. Visible light promoted degradation of gaseous volatile organic compounds catalyzed by Au supported layered double hydroxides: influencing factors, kinetics and mechanism. J. Hazard. Mater. 363, 41–54.

Fu, Y., Xu, P., Huang, D., Zeng, G., Lai, C., Qin, L., Li, B., He, J., Yi, H., Cheng, M., Zhang, C., 2019c. Au nanoparticles decorated on activated coke via a facile preparation for efficient catalytic reduction of nitrophenols and azo dyes. Appl. Surf. Sci. 473, 578–588.

Fu, Y., Zeng, G., Lai, C., Huang, D., Qin, L., Yi, H., Liu, X., Zhang, M., Li, B., Liu, S., Li, L., Li, M., Wang, W., Zhang, Y., Pi, Z., 2020. Hybrid architectures based on noble metals and carbon-based dots nanomaterials: a review of recent progress in synthesis and applications. Chem. Eng. J. 399, 125743.

Fuku, K., Hayashi, R., Takakura, S., Kamegawa, T., Mori, K., Yamashita, H., 2013. The synthesis of size- and color-controlled silver nanoparticles by using microwave heating and their enhanced catalytic activity by localized surface plasmon resonance. Angew. Chem. 125 (29), 7594–7598.

Gao, X., Liu, X., Zhu, Z., Gao, Y., Wang, Q., Zhu, F., Xie, Z., 2017. Enhanced visible light photocatalytic performance of CdS sensitized TiO 2 nanorod arrays decorated with Au nanoparticles as electron sinks. Sci. Rep. 7 (1), 973.

Gautam, P., Kumar, S., Lokhandwala, S., 2019. Advanced oxidation processes for treatment of leachate from hazardous waste landfill: a critical review. J. Clean. Prod. 237, 117639.

Georgi, A., Velasco Polo, M., Crincoli, K., Mackenzie, K., Kopinke, F.-D., 2016. Accelerated catalytic Fenton reaction with traces of iron: an Fe–Pd-multicatalysis approach. Environ. Sci. Technol. 50 (11), 5882–5891.

Godoi, D.R.M., Villullas, H.M., Zhu, F.-C., Jiang, Y.-X., Sun, S.-G., Guo, J., Sun, L., Chen, R., 2016. A comparative investigation of metal-support interactions on the catalytic activity of Pt nanoparticles for ethanol oxidation in alkaline medium. J. Power Sources 311, 81–90.

Gołąbiewska, A., Malankowska, A., Jarek, M., Lisowski, W., Nowaczyk, G., Jurga, S., Zaleska-Medynska, A., 2016. The effect of gold shape and size on the properties and visible light-induced photoactivity of Au-TiO2. Appl. Catal. B: Environ. 196, 27–40.

Guo, J.-Z., Cui, H., Zhou, W., Wang, W., 2008. Ag nanoparticle-catalyzed chemiluminescent reaction between luminol and hydrogen peroxide. J. Photochem. Photobiol. A: Chem. 193 (2), 89–96.

Han, Y.-F., Phonthammachai, N., Ramesh, K., Zhong, Z., White, T., 2008. Removing organic compounds from aqueous medium via wet peroxidation by gold catalysts. Environ. Sci. Technol. 42 (3), 908–912.

He, D., Jones, A.M., Garg, S., Pham, A.N., Waite, T.D., 2011. Silver nanoparticle–reactive oxygen species interactions: application of a charging–discharging model. J. Phys. Chem. C 115 (13), 5461–5468.
He, D., Garg, S., Waite, T.D., 2012. H2O2-mediated oxidation of zero-valent silver and resultant interactions among silver nanoparticles, silver ions, and reactive oxygen species. Langmuir 28 (27), 10266–10275.
He, D., Miller, C.J., Waite, T.D., 2014. Fenton-like zero-valent silver nanoparticle-mediated hydroxyl radical production. J. Catal. 317, 198–205.
He, D., Niu, H., He, S., Mao, L., Cai, Y., Liang, Y., 2019. Strengthened Fenton degradation of phenol catalyzed by core/shell Fe–Pd@C nanocomposites derived from mechanochemically synthesized Fe-Metal organic frameworks. Water Res. 162, 151–160.
He, J., Lai, C., Qin, L., Li, B., Liu, S., Jiao, L., Fu, Y., Huang, D., Li, L., Zhang, M., Liu, X., Yi, H., Chen, L., Li, Z., 2020. Strategy to improve gold nanoparticles loading efficiency on defect-free high silica ZSM-5 zeolite for the reduction of nitrophenols. Chemosphere 256, 127083.
He, K., Zeng, Z., Chen, A., Zeng, G., Xiao, R., Xu, P., Huang, Z., Shi, J., Hu, L., Chen, G., 2018. Advancement of Ag–graphene based nanocomposites: an overview of synthesis and its applications. Small 14 (32), 1800871.
Hodges, B.C., Cates, E.L., Kim, J.-H., 2018. Challenges and prospects of advanced oxidation water treatment processes using catalytic nanomaterials. Nat. Nanotechnol. 13 (8), 642–650.
Hu, C., Ting, S.-W., Chan, K.-Y., Huang, W., 2012. Reaction pathways derived from DFT for understanding catalytic decomposition of formic acid into hydrogen on noble metals. Int. J. Hydrog. Energy 37 (21), 15956–15965.
Hu, G., Huang, Z.-P., Hu, C.-X., Zhang, Z.-Q., Liu, R.-T., Li, X.-Y., Zhang, L., Wang, Q., Zhang, H.-L., 2020. Selective photocatalytic hydrogenation of α,β-unsaturated aldehydes on Au/CuCo2O4 nanotubes under visible-light irradiation. ACS Sustain. Chem. Eng. 8 (22), 8288–8294.
Huang, B., Qi, C., Yang, Z., Guo, Q., Chen, W., Zeng, G., Lei, C., 2017. Pd/Fe3O4 nanocatalysts for highly effective and simultaneous removal of humic acids and Cr (VI) by electro-Fenton with H2O2 in situ electro-generated on the catalyst surface. J. Catal. 352, 337–350.
Huang, X., El-Sayed, I.H., Qian, W., El-Sayed, M.A., 2006. Cancer cell imaging and photothermal therapy in the near-infrared region by using gold nanorods. J. Am. Chem. Soc. 128 (6), 2115–2120.
Huang, Y., Liu, H., Liu, S., Li, C., Yuan, S., 2020a. Glucose oxidase modified Fenton reactions for in-situ ROS generation and potential application in groundwater remediation. Chemosphere 253, 126648.
Huang, Z., Zeng, Z., Song, Z., Chen, A., Zeng, G., Xiao, R., He, K., Yuan, L., Li, H., Chen, G., 2020b. Antimicrobial efficacy and mechanisms of silver nanoparticles against Phanerochaete chrysosporium in the presence of common electrolytes and humic acid. J. Hazard. Mater. 383, 121153.
Huerta-Aguilar, C.A., Ramírez-Alejandre, A.A., Thangarasu, P., Arenas-Alatorre, J.A., Reyes-Dominguez, I.A., de la Luz Corea, M., 2019. Cystal phase induced band gap energy enhancing the photo-catalytic properties of Zn–Fe2O4/Au NPs: experimental and theoretical studies. Catal. Sci. Technol. 9 (12), 3066–3080.
Ibrahim, M., Labaki, M., Giraudon, J.-M., Lamonier, J.-F., 2020. Hydroxyapatite, a multifunctional material for air, water and soil pollution control: a review. J. Hazard. Mater. 383, 121139.
Ismail, A.A., Bahnemann, D.W., Bannat, I., Wark, M., 2009. Gold nanoparticles on mesoporous interparticle networks of titanium dioxide nanocrystals for enhanced photonic efficiencies. J. Phys. Chem. C 113 (17), 7429–7435.
Jiang, G., Lan, M., Zhang, Z., Lv, X., Lou, Z., Xu, X., Dong, F., Zhang, S., 2017. Identification of active hydrogen species on palladium nanoparticles for an enhanced electrocatalytic hydrodechlorination of 2,4-dichlorophenol in water. Environ. Sci. Technol. 51 (13), 7599–7605.
Jiang, J., Song, Y., Wang, X., Li, T., Li, M., Lin, Y., Xie, T., Dong, S., 2020. Enhancing aqueous pollutant photodegradation via a Fermi level matched Z-scheme BiOI/Pt/g-C3N4 photocatalyst: unobstructed photogenerated charge behavior and degradation pathway exploration. Catal. Sci. Technol. 10 (10), 3324–3333.
Jiang, W., Bai, S., Wang, L., Wang, X., Yang, L., Li, Y., Liu, D., Wang, X., Li, Z., Jiang, J., Xiong, Y., 2016. Integration of multiple plasmonic and co-catalyst nanostructures on TiO2 nanosheets for visible-near-infrared photocatalytic hydrogen evolution. Small 12 (12), 1640–1648.
Jiang, Z., Ouyang, Q., Peng, B., Zhang, Y., Zan, L., 2014. Ag size-dependent visible-light-responsive photoactivity of Ag–TiO2 nanostructure based on surface plasmon resonance. J. Mater. Chem. A 2 (46), 19861–19866.
Jiang, Z., Jiang, D., Wei, W., Yan, Z., Xie, J., 2015. Natural carbon nanodots assisted development of size-tunable metal (Pd, Ag) nanoparticles grafted on bionic dendritic α-Fe2O3 for cooperative catalytic applications. J. Mater. Chem. A 3 (46), 23607–23620.
Jin, R., Zeng, C., Zhou, M., Chen, Y., 2016. Atomically precise colloidal metal nanoclusters and nanoparticles: fundamentals and opportunities. Chem. Rev. 10346.
Jones, A.M., Garg, S., He, D., Pham, A.N., Waite, T.D., 2011. Superoxide-mediated formation and charging of silver nanoparticles. Environ. Sci. Technol. 45 (4), 1428–1434.
Ju, P., Wang, Y., Sun, Y., Zhang, D., 2020. In-situ green topotactic synthesis of a novel Z-scheme Ag@AgVO3/BiVO4 heterostructure with highly enhanced visible-light photocatalytic activity. J. Colloid Interface Sci. 579, 431–447.
Kamarudin, N.S., Jusoh, R., Sukor, N.F., Jalil, A.A., Setiabudi, H.D., Salleh, N.F.M., 2021. Facile electro-assisted green synthesis of size-tunable silver nanoparticles and its photodegradation activity. J. Clust. Sci.
Kavitha, R., Nithya, P.M., Girish Kumar, S., 2020. Noble metal deposited graphitic carbon nitride based heterojunction photocatalysts. Appl. Surf. Sci. 508, 145142.
Kiyonaga, T., Jin, Q., Kobayashi, H., Tada, H., 2009. Size-dependence of catalytic activity of gold nanoparticles loaded on titanium (IV) dioxide for hydrogen peroxide decomposition. ChemPhysChem 10 (17), 2935–2938.
Lai, C., Zhang, M., Li, B., Huang, D., Zeng, G., Qin, L., Liu, X., Yi, H., Cheng, M., Li, L., Chen, Z., Chen, L., 2019. Fabrication of CuS/BiVO4 (0 4 0) binary heterojunction photocatalysts with enhanced photocatalytic activity for Ciprofloxacin degradation and mechanism insight. Chem. Eng. J. 358, 891–902.
Lang, Q., Chen, Y., Huang, T., Yang, L., Zhong, S., Wu, L., Chen, J., Bai, S., 2018. Graphene "bridge" in transferring hot electrons from plasmonic Ag nanocubes to TiO2 nanosheets for enhanced visible light photocatalytic hydrogen evolution. Appl. Catal. B: Environ. 220, 182–190.
Lee, J.E., Bera, S., Choi, Y.S., Lee, W.I., 2017. Size-dependent plasmonic effects of M and M@SiO2 (M = Au or Ag) deposited on TiO2 in photocatalytic oxidation reactions. Appl. Catal. B: Environ. 214, 15–22.
Li, B., Lai, C., Zeng, G., Huang, D., Qin, L., Zhang, M., Cheng, M., Liu, X., Yi, H., Zhou, C., Huang, F., Liu, S., Fu, Y., 2019a. Black phosphorus, a rising star 2D nanomaterial in the post-graphene era: synthesis, properties, modifications, and photocatalysis applications. Small 15 (8), 1804565.
Li, B., Liu, S., Lai, C., Zeng, G., Zhang, M., Zhou, M., Huang, D., Qin, L., Liu, X., Li, Z., An, N., Xu, F., Yi, H., Zhang, Y., Chen, L., 2020a. Unravelling the interfacial charge migration pathway at atomic level in 2D/2D interfacial Schottky heterojunction for visible-light-driven molecular oxygen activation. Appl. Catal. B: Environ. 266, 118650.
Li, H., Bian, Z., Zhu, J., Huo, Y., Li, H., Lu, Y., 2007. Mesoporous Au/TiO2 nanocomposites with enhanced photocatalytic activity. J. Am. Chem. Soc. 129 (15), 4538–4539.
Li, H., Shen, L., Zhang, K., Sun, B., Ren, L., Qiao, P., Pan, K., Wang, L., Zhou, W., 2018b. Surface plasmon resonance-enhanced solar-driven photocatalytic performance from Ag nanoparticle-decorated self-floating porous black TiO2 foams. Appl. Catal. B: Environ. 220, 111–117.
Li, J., Cushing, S.K., Bright, J., Meng, F., Senty, T.R., Zheng, P., Bristow, A.D., Wu, N., 2013. Ag@Cu2O core-shell nanoparticles as visible-light plasmonic photocatalysts. ACS Catal. 3 (1), 47–51.
Li, J., Yuan, H., Zhu, Z., 2015a. Fabrication of Cu2O/Au/BiPO4 Z-scheme photocatalyst to improve the photocatalytic activity under solar light. J. Mol. Catal. A: Chem. 410, 133–139.
Li, L., Lai, C., Huang, F., Cheng, M., Zeng, G., Huang, D., Li, B., Liu, S., Zhang, M., Qin, L., Li, M., He, J., Zhang, Y., Chen, L., 2019b. Degradation of naphthalene with magnetic bio-char activate hydrogen peroxide: Synergism of bio-char and Fe–Mn binary oxides. Water Res. 160, 238–248.
Li, M., Yu, Z., Liu, Q., Sun, L., Huang, W., 2016. Photocatalytic decomposition of perfluorooctanoic acid by noble metallic nanoparticles modified TiO2. Chem. Eng. J. 286, 232–238.
Li, N., Zhao, P., Astruc, D., 2014. Anisotropic gold nanoparticles: synthesis, properties, applications, and toxicity. Angew. Chem. 53, 7.
Li, Nan, Wu, Jiaojiao, Fang, Hua-Bin, Zhang, Xiao-Hong, Zheng, Yan-Zhen, 2018a. Au-nanorod-anchored {001} facets of Bi4Ti3O12 nanosheets for enhanced visible-light-driven photocatalysis. Appl. Surf. Sci.
Li, S., Cai, J., Wu, X., Zheng, F., 2018c. Sandwich-like TiO2@ZnO-based noble metal (Ag, Au, Pt, or Pd) for better photo-oxidation performance: Synergistic effect between noble metal and metal oxide phases. Appl. Surf. Sci. 443, 603–612.
Li, X., Liu, X., Xu, L., Wen, Y., Ma, J., Wu, Z., 2015b. Highly dispersed Pd/PdO/Fe2O3 nanoparticles in SBA-15 for Fenton-like processes: confinement and synergistic effects. Appl. Catal. B: Environ. 165, 79–86.
Li, X., Zeng, Z., Zeng, G., Wang, D., Xiao, R., Wang, Y., Zhou, C., Yi, H., Ye, S., Yang, Y., Xiong, W., 2020b. A "bottle-around-ship" like method synthesized yolk-shell Ag3PO4@MIL-53(Fe) Z-scheme photocatalysts for enhanced tetracycline removal. J. Colloid Interface Sci. 561, 501–511.
Liang, X., Wang, P., Gao, Y., Huang, H., Tong, F., Zhang, Q., Wang, Z., Liu, Y., Zheng, Z., Dai, Y., Huang, B., 2020. Design and synthesis of porous M-ZnO/CeO2 microspheres as efficient plasmonic photocatalysts for nonpolar gaseous molecules oxidation: insight into the role of oxygen vacancy defects and M=Ag. Au Nanopart. Appl. Catal. B: Environ. 260, 118151.
Liang, Y., Li, J., He, Y., Jiang, Z., Shangguan, W., 2021. Catalytic oxidation of dimethyl phthalate over titania-supported noble metal catalysts. J. Hazard. Mater. 401, 123274.
Liao, P., Yuan, S., Chen, M., Tong, M., Xie, W., Zhang, P., 2013. Regulation of electrochemically generated ferrous ions from an iron cathode for Pd-catalytic transformation of MTBE in groundwater. Environ. Sci. Technol. 47 (14), 7918–7926.
Liao, P., Al-Ani, Y., Ismael, Z.M., Wu, X., 2015. Insights into the role of humic acid on Pd-catalytic electro-Fenton transformation of toluene in groundwater. Sci. Rep. 5, 9239.
Liao, Z., Dai, S., Long, S., Yu, Y., Ali, J., Wang, H., Chen, Z., Chen, Z., 2018. Pd based in situ AOPs with heterogeneous catalyst of FeMgAl layered double hydrotalcite for the degradation of bisphenol A and landfill leachate through multiple pathways. Environ. Sci. Pollut. Res. Int. 25 (35), 35623–35636.
Liotta, L.F., Gruttadauria, M., Di Carlo, G., Perrini, G., Librando, V., 2009. Heterogeneous catalytic degradation of phenolic substrates: catalysts activity. J. Hazard. Mater. 162 (2), 588–606.
Liu, F., Liu, Y., Yao, Q., Wang, Y., Fang, X., Shen, C., Li, F., Huang, M., Wang, Z., Sand, W., Xie, J., 2020a. Supported atomically-precise gold nanoclusters for enhanced flow-through electro-Fenton. Environ. Sci. Technol. 54 (9), 5913–5921.
Liu, G., Huang, Y., Lv, H., Wang, H., Zeng, Y., Yuan, M., Meng, Q., Wang, C., 2021. Confining single-atom Pd on g-C3N4 with carbon vacancies towards enhanced photocatalytic NO conversion. Appl. Catal. B: Environ. 284, 119683.
Liu, J., Feng, J., Gui, J., Chen, T., Xu, M., Wang, H., Dong, H., Chen, H., Li, X., Wang, L., Chen, Z., Yang, Z., Liu, J., Hao, W., Yao, Y., Gu, L., Weng, Y., Huang, Y., Duan, X.,

Zhang, J., Li, Y., 2018a. Metal@semiconductor core-shell nanocrystals with atomically organized interfaces for efficient hot electron-mediated photocatalysis. Nano Energy 48, 44–52.
Liu, J., Ma, Q., Huang, Z., Liu, G., Zhang, H., 2019a. Recent progress in graphene-based noble-metal nanocomposites for electrocatalytic applications. Adv. Mater. 31 (9), 1800696.
Liu, L., Zhang, X., Yang, L., Ren, L., Wang, D., Ye, J., 2017a. Metal nanoparticles induced photocatalysis. Natl. Sci. Rev. 4 (5), 761–780.
Liu, L., Zakharov, D.N., Arenal, R., Concepcion, P., Stach, E.A., Corma, A., 2018b. Evolution and stabilization of subnanometric metal species in confined space by in situ TEM. Nat. Commun. 9, 1.
Liu, S., Lai, C., Li, B., Zhang, C., Zhang, M., Huang, D., Qin, L., Yi, H., Liu, X., Huang, F., Zhou, X., Chen, L., 2020b. Role of radical and non-radical pathway in activating persulfate for degradation of p-nitrophenol by sulfur-doped ordered mesoporous carbon. Chem. Eng. J. 384, 123304.
Liu, X., Iocozzia, J., Wang, Y., Cui, X., Chen, Y., Zhao, S., Li, Z., Lin, Z., 2017b. Noble metal–metal oxide nanohybrids with tailored nanostructures for efficient solar energy conversion, photocatalysis and environmental remediation. Energy Environ. Sci. 10 (2), 402–434.
Liu, X., Chen, L., Zhu, T., Ning, R., 2019a. Catalytic oxidation of chlorobenzene over noble metals (Pd, Pt, Ru, Rh) and the distributions of polychlorinated by-products. J. Hazard Mater. 363, 90–98.
Liu, X., Fan, J.H., Liu, Z.X., Yu, Y., You, J.J., Zhu, X.Q., Zhong, X.X., Ma, S.J., Lin, Z.X., 2019b. Elimination of 4-chlorophenol in aqueous solution by the novel Pd/MIL-101 (Cr)-hydrogen-accelerated catalytic Fenton system. Appl. Organomet. Chem. 33, 11.
Liu, X., Gao, S.-Q., Fan, J.-H., Li, X.-M., Qin, H.-H., Wang, J.-X., Ma, S.-J., Liu, Z.-X., Yu, Y., 2019c. The construction of accelerated catalytic Fenton reaction based on Pd/MIL-101(Cr) and H2. New J. Chem. 43 (21), 8179–8188.
Liu, X., Huang, D., Lai, C., Zeng, G., Qin, L., Wang, H., Yi, H., Li, B., Liu, S., Zhang, M., Deng, R., Fu, Y., Li, L., Xue, W., Chen, S., 2019d. Recent advances in covalent organic frameworks (COFs) as a smart sensing material. Chem. Soc. Rev.
Liu, Y., Zhao, Y., Fan, Q., Khan, M.S., Li, X., Zhang, Y., Ma, H., Wei, Q., 2018c. Aptamer based electrochemiluminescent thrombin assay using carbon dots anchored onto silver-decorated polydopamine nanospheres. Mikrochim. Acta 185 (2), 85.
Low, J., Jiang, C., Cheng, B., Wageh, S., Al-Ghamdi, A.A., Yu, J., 2017. A review of direct Z-scheme photocatalysts. Small Methods 1 (5), 1700080.
Luo, H., Zeng, Z., Zeng, G., Zhang, C., Xiao, R., Huang, D., Lai, C., Cheng, M., Wang, W., Xiong, W., Yang, Y., Qin, L., Zhou, C., Wang, H., Zhou, Y., Tian, S., 2020a. Recent progress on metal-organic frameworks based- and derived-photocatalysts for water splitting. Chem. Eng. J. 383, 123196.
Luo, M., Yuan, S., Tong, M., Liao, P., Xie, W., Xu, X., 2014. An integrated catalyst of Pd supported on magnetic Fe3O4 nanoparticles: simultaneous production of H2O2 and Fe2+ for efficient electro-Fenton degradation of organic contaminants. Water Res. 48, 190–199.
Luo, S., Zeng, Z., Zeng, G., Liu, Z., Xiao, R., Xu, P., Wang, H., Huang, D., Liu, Y., Shao, B., Liang, Q., Wang, D., He, Q., Qin, L., Fu, Y., 2020b. Recent advances in conjugated microporous polymers for photocatalysis: designs, applications, and prospects. J. Mater. Chem. A 8 (14), 6434–6470.
Ma, X., Sun, H., Wang, Y., Wu, X., Zhang, J., 2018. Electronic and optical properties of strained noble metals: Implications for applications based on LSPR. Nano Energy 53, 932–939.
Ma, Y., Wu, X., Zhang, G., 2017. Core-shell Ag@Pt nanoparticles supported on sepiolite nanofibers for the catalytic reduction of nitrophenols in water: enhanced catalytic performance and DFT study. Appl. Catal. B: Environ. 205, 262–270.
Mantzavinos, D., Poulios, I., 2010. Preface. Catal. Today 151 (1), 1.
Martín, R., Navalon, S., Alvaro, M., Garcia, H., 2011. Optimized water treatment by combining catalytic Fenton reaction using diamond supported gold and biological degradation. Appl. Catal. B: Environ. 103 (1), 246–252.
Meng, A., Zhang, L., Cheng, B., Yu, J., 2019a. Dual cocatalysts in TiO2 photocatalysis. Adv. Mater. 31 (30), e1807660.
Meng, A., Zhang, L., Cheng, B., Yu, J., 2019b. Dual cocatalysts in TiO2 photocatalysis. Adv. Mater. 31 (30), 1807660.
Meng, X., Zong, P., Wang, L., Yang, F., Hou, W., Zhang, S., Li, B., Guo, Z., Liu, S., Zuo, G., Du, Y., Wang, T., Roy, V.A.L., 2020. Au-nanoparticle-supported ZnO as highly efficient photocatalyst for H2O2 production. Catal. Commun. 134, 105860.
Mishra, P., Patnaik, S., Parida, K., 2019. An overview of recent progress on noble metal modified magnetic Fe3O4 for photocatalytic pollutant degradation and H2 evolution. Catal. Sci. Technol. 9 (4), 916–941.
Misra, M., Chowdhury, S.R., Lee, T.I., 2020. Sunlight driven decomposition of toxic organic compound, coumarin, p-nitrophenol, and photo reduction of Cr(VI) ions, using a bridge structure of Au@CNT@TiO2 nanocomposite. Appl. Catal. B: Environ. 272, 118991.
Mittal, M., Gupta, A., Pandey, O.P., 2018. Role of oxygen vacancies in Ag/Au doped CeO2 nanoparticles for fast photocatalysis. Sol. Energy 165, 206–216.
Nan, B., Hu, X.-C., Wang, X., Jia, C.-J., Ma, C., Li, M.-X., Si, R., 2017. Effects of multiple platinum species on catalytic reactivity distinguished by electron microscopy and x-ray absorption spectroscopy techniques. J. Phys. Chem. C 121 (46), 25805–25817.
Nasr, O., Mohamed, O., Al-Shirbini, A.-S., Abdel-Wahab, A.-M., 2019. Photocatalytic degradation of acetaminophen over Ag, Au and Pt loaded TiO2 using solar light. J. Photochem. Photobiol. A: Chem. 374, 185–193.
Navalon, S., Martin, R., Alvaro, M., Garcia, H., 2010. Gold on diamond nanoparticles as a highly efficient Fenton catalyst. Angew. Chem. Int. Ed. 49 (45), 8403–8407.
Navalon, S., de Miguel, M., Martin, R., Alvaro, M., Garcia, H., 2011. Enhancement of the catalytic activity of supported gold nanoparticles for the Fenton reaction by light. J. Am. Chem. Soc. 133 (7), 2218–2226.
Naya, S.-i, Teranishi, M., Kimura, K., Tada, H., 2011. A strong support-effect on the catalytic activity of gold nanoparticles for hydrogen peroxide decomposition. Chem. Commun. 47 (11), 3230–3232.
Niu, H., Zheng, Y., Wang, S., Zhao, L., Yang, S., Cai, Y., 2018. Continuous generation of hydroxyl radicals for highly efficient elimination of chlorophenols and phenols catalyzed by heterogeneous Fenton-like catalysts yolk/shell Pd@Fe3O4@metal organic frameworks. J. Hazard. Mater. 346, 174–183.
Nogueira, R.F.P., Oliveira, M.C., Paterlini, W.C., 2005. Simple and fast spectrophotometric determination of H2O2 in photo-Fenton reactions using metavanadate. Talanta 66 (1), 86–91.
Osajima, J.A., Sá, A.S., Honorio, L.M.C., Trigueiro, P., Pinto, L.I.F., Oliveira, J.A., Furtini, M.B., Bezerra, R.D.S., Alcantara, A.C.S., Silva-Filho, E.C., 2021. Au@Ag bimetallic nanoparticles deposited on palygorskite in the presence of TiO2 for enhanced photodegradation activity through synergistic effect. Environ. Sci. Pollut. Res. 28 (19), 23995–24007.
Patnaik, S., Sahoo, D.P., Parida, K.M., 2020. Bimetallic co-effect of Au-Pd alloyed nanoparticles on mesoporous silica modified g-C3N4 for single and simultaneous photocatalytic oxidation of phenol and reduction of hexavalent chromium. J. Colloid Interface Sci. 560, 519–535.
Peng, S.-Y., Yang, L., Yu, L., Li, X.-Y., Zhou, Y.-Z., Lv, Y., Zhu, F., 2019. Well-defined Pd anchoring on the surface of porous ZnO nanocomposites with excellent photocatalytic activity and good reusability for the removal of phenol from water. New J. Chem. 43 (46), 18034–18040.
Pi, L., Cai, J., Xiong, L., Cui, J., Hua, H., Tang, D., Mao, X., 2020. Generation of H2O2 by on-site activation of molecular dioxygen for environmental remediation applications: a review. Chem. Eng. J. 389, 123420.
Pozzo, M., Alfè, D., 2009. Hydrogen dissociation and diffusion on transition metal (=Ti, Zr, V, Fe, Ru, Co, Rh, Ni, Pd, Cu, Ag)-doped Mg(0001) surfaces. Int. J. Hydrog. Energy 34 (4), 1922–1930.
Pulido Melián, E., González Díaz, O., Doña Rodríguez, J.M., Colón, G., Navío, J.A., Macías, M., Pérez Peña, J., 2012. Effect of deposition of silver on structural characteristics and photoactivity of TiO2-based photocatalysts. Appl. Catal. B: Environ. 127, 112–120.
Qin, L., Zeng, G., Lai, C., Huang, D., Xu, P., Zhang, C., Cheng, M., Liu, X., Liu, S., Li, B., Yi, H., 2018. "Gold rush" in modern science: fabrication strategies and typical advanced applications of gold nanoparticles in sensing. Coord. Chem. Rev. 359, 1–31.
Qin, L., Yi, H., Zeng, G., Lai, C., Huang, D., Xu, P., Fu, Y., He, J., Li, B., Zhang, C., Cheng, M., Wang, H., Liu, X., 2019a. Hierarchical porous carbon material restricted Au catalyst for highly catalytic reduction of nitroaromatics. J. Hazard. Mater. 380, 120864.
Qin, L., Zeng, G., Lai, C., Huang, D., Zhang, C., Cheng, M., Yi, H., Liu, X., Zhou, C., Xiong, W., Huang, F., Cao, W., 2019b. Synthetic strategies and application of gold-based nanocatalysts for nitroaromatics reduction. Sci. Total Environ. 652, 93–116.
Qin, L., Zeng, Z., Zeng, G., Lai, C., Duan, A., Xiao, R., Huang, D., Fu, Y., Yi, H., Li, B., Liu, X., Liu, S., Zhang, M., Jiang, D., 2019c. Cooperative catalytic performance of bimetallic Ni-Au nanocatalyst for highly efficient hydrogenation of nitroaromatics and corresponding mechanism insight. Appl. Catal. B: Environ. 259, 118035.
Qin, L., Wang, Z., Fu, Y., Lai, C., Liu, X., Li, B., Liu, S., Yi, H., Li, L., Zhang, M., Li, Z., Cao, W., Niu, Q., 2021. Gold nanoparticles-modified MnFe2O4 with synergistic catalysis for photo-Fenton degradation of tetracycline under neutral pH. J. Hazard. Mater. 414, 125448.
Qin, Y., Sun, M., Liu, H., Qu, J., 2015. AuPd/Fe3O4-based three-dimensional electrochemical system for efficiently catalytic degradation of 1-butyl-3-methylimidazolium hexafluorophosphate. Electrochim. Acta 186, 328–336.
Qiu, J., Zhang, X., Xie, K., Zhang, X.-F., Feng, Y., Jia, M., Yao, J., 2019. Noble metal nanoparticle-functionalized Zr-metal organic frameworks with excellent photocatalytic performance. J. Colloid Interface Sci. 538, 569–577.
Quintanilla, A., García-Rodríguez, S., Domínguez, C.M., Blasco, S., Casas, J.A., Rodriguez, J.J., 2012. Supported gold nanoparticle catalysts for wet peroxide oxidation. Appl. Catal. B: Environ. 111–112, 81–89.
Rani, A., Patel, A.S., Chakraborti, A., Singh, K., Sharma, P., 2021. Enhanced photocatalytic activity of plasmonic Au nanoparticles incorporated MoS2 nanosheets for degradation of organic dyes. J. Mater. Sci.: Mater. Electron. 32 (5), 6168–6184.
Reyes-Cruzaley, A.P., Félix-Navarro, R.M., Trujillo-Navarrete, B., Silva-Carrillo, C., Zapata-Fernández, J.R., Romo-Herrera, J.M., Contreras, O.E., Reynoso-Soto, E.A., 2019. Synthesis of novel Pd NP-PTH-CNTs hybrid material as catalyst for H2O2 generation. Electrochim. Acta 296, 575–581.
Sha, J., Zheng, E.-J., Zhou, W.-J., Liebens, A., Pera-Titus, M., 2016. Selective oxidation of fatty alcohol ethoxylates with H2O2 over Au catalysts for the synthesis of alkyl ether carboxylic acids in alkaline solution. J. Catal. 337, 199–207.
Shang, C., Liu, Z.P., 2011. Origin and activity of gold nanoparticles as aerobic oxidation catalysts in aqueous solution. J. Am. Chem. Soc. 133 (25), 9938–9947.
Shen, M., Zhang, Y., Zhu, Y., Song, B., Zeng, G., Hu, D., Wen, X., Ren, X., 2019a. Recent advances in toxicological research of nanoplastics in the environment: a review. Environ. Pollut. 252, 511–521.
Shen, M., Song, B., Zhu, Y., Zeng, G., Zhang, Y., Yang, Y., Wen, X., Chen, M., Yi, H., 2020. Removal of microplastics via drinking water treatment: current knowledge and future directions. Chemosphere 251, 126612.
Shen, R., Chen, W., Peng, Q., Lu, S., Zheng, L., Cao, X., Wang, Y., Zhu, W., Zhang, J., Zhuang, Z., Chen, C., Wang, D., Li, Y., 2019b. High-concentration single atomic Pt sites on hollow CuSx for selective O2 reduction to H2O2 in acid solution. Chem 5 (8), 2099–2110.
Song, B., Gong, J., Tang, W., Zeng, G., Chen, M., Xu, P., Shen, M., Ye, S., Feng, H., Zhou, C., Yang, Y., 2020a. Influence of multi-walled carbon nanotubes on the

microbial biomass, enzyme activity, and bacterial community structure in 2,4-dichlorophenol-contaminated sediment. Sci. Total Environ. 713, 136645.
Song, B., Zeng, Z., Zeng, G., Gong, J., Xiao, R., Chen, M., Tang, X., Ye, S., Shen, M., 2021. Effects of hydroxyl, carboxyl, and amino functionalized carbon nanotubes on the functional diversity of microbial community in riverine sediment. Chemosphere 262, 128053.
Song, C., Li, X., Zhang, L., Yan, P., Xu, C., Zhu, K., Cheng, K., Ye, K., Yan, J., Cao, D., Wang, G., 2020b. Pd nanoparticles anchored to nano-peony CoMn2O4 as an efficient catalyst for H2O2 electroreduction. J. Electroanal. Chem. 858, 113711.
Song, H., Wei, L., Chen, C., Wen, C., Han, F., 2019a. Photocatalytic production of H2O2 and its in situ utilization over atomic-scale Au modified MoS2 nanosheets. J. Catal. 376, 198–208.
Song, M., Wu, Y., Xu, C., Wang, X., Su, Y., 2019b. Synergistic effects of multi-active sites in silver modified Bi degrees-BiVO4 toward efficient reduction of aromatic nitrobenzene. J. Hazard Mater. 368, 530–540.
Subramanian, V., Wolf, E., Kamat, P.V., 2001. Semiconductor–metal composite nanostructures. To what extent do metal nanoparticles improve the photocatalytic activity of TiO2 films? J. Phys. Chem. B.
Suh, M., Bagus, P.S., Pak, S., Rosynek, M.P., Lunsford, J.H., 2000. Reactions of hydroxyl radicals on titania, silica, alumina, and gold surfaces. J. Phys. Chem. B 104 (12), 2736–2742.
Sun, D., Zhang, Y., Liu, Y., Wang, Z., Chen, X., Meng, Z., Kang, S., Zheng, Y., Cui, L., Chen, M., Dong, M., Hu, B., 2020a. In-situ homodispersely immobilization of Ag@AgCl on chloridized g-C3N4 nanosheets as an ultrastable plasmonic photocatalyst. Chem. Eng. J. 384, 123259.
Sun, M., Zhang, G., Liu, Y., Liu, H., Qu, J., Li, J., 2015. Highly efficient AuPd/carbon nanotube nanocatalysts for the electro-Fenton process. Chem. – Eur. J. 21 (20), 7611–7620.
Sun, Y., Zhu, Q., Bai, B., Li, Y., He, C., 2020b. Novel all-solid-state Z-scheme SnO2/Pt/In2O3 photocatalyst with boosted photocatalytic performance on water splitting and 2,4-dichlorophenol degradation under visible light. Chem. Eng. J. 390, 124518.
Tan, T.-Y., Zeng, Z.-T., Zeng, G.-M., Gong, J.-L., Xiao, R., Zhang, P., Song, B., Tang, W.-W., Ren, X.-Y., 2020. Electrochemically enhanced simultaneous degradation of sulfamethoxazole, ciprofloxacin and amoxicillin from aqueous solution by multi-walled carbon nanotube filter. Sep. Purif. Technol. 235, 116167.
Teixeira, I.F., Barbosa, E.C.M., Tsang, S.C.E., Camargo, P.H.C., 2018. Carbon nitrides and metal nanoparticles: from controlled synthesis to design principles for improved photocatalysis. Chem. Soc. Rev. 47 (20), 7783–7817.
Tong, T., Zhu, B., Jiang, C., Cheng, B., Yu, J., 2018. Mechanistic insight into the enhanced photocatalytic activity of single-atom Pt, Pd or Au-embedded g-C3N4. Appl. Surf. Sci. 433, 1175–1183.
Tou, A., Kim, H.-H., Einaga, H., Teramoto, Y., Ogata, A., 2019. Ozone-assisted catalysis of CO: in situ Fourier transform IR evidence of the cooperative effect of a bimetallic Ag-Pd catalyst. Chem. Eng. J. 355, 380–389.
Trabelsi, K., Hajjaji, A., Gaidi, M., Bessais, B., El Khakani, M.A., 2017. Enhancing the photoelectrochemical response of TiO2nanotubes through their nanodecoration by pulsed-laser-deposited Ag nanoparticles. J. Appl. Phys. 122 (6), 064503.
Trang, T.N.Q., Phan, T.B., Nam, N.D., Thu, V.T.H., 2020. In situ charge transfer at the Ag@ZnO photoelectrochemical interface toward the high photocatalytic performance of H2 evolution and RhB degradation. ACS Appl. Mater. Interfaces.
Vaiano, V., Jaramillo-Paez, C.A., Matarangolo, M., Navío, J.A., del Carmen Hidalgo, M., 2019. UV and visible-light driven photocatalytic removal of caffeine using ZnO modified with different noble metals (Pt, Ag and Au). Mater. Res. Bull. 112, 251–260.
Wang, B., Cai, H., Shen, S., 2019a. Single metal atom photocatalysis. Small Methods 3 (9), 1800447.
Wang, C., Astruc, D., 2014. Nanogold plasmonic photocatalysis for organic synthesis and clean energy conversion. Chem. Soc. Rev. 43 (20), 7188–7216.
Wang, C., Astruc, D., 2015. Nanogold plasmonic photocatalysis for organic synthesis and clean energy conversion. Chem. Soc. Rev. 45 (50), 7188–7216.
Wang, H., Wang, H., Wang, Z., Tang, L., Zeng, G., Xu, P., Chen, M., Xiong, T., Zhou, C., Li, X., Huang, D., Zhu, Y., Wang, Z., Tang, J., 2020. Covalent organic framework photocatalysts: structures and applications. Chem. Soc. Rev. 49 (12), 4135–4165.
Wang, K., Li, J., Zhang, G., 2019b. Ag-bridged Z-scheme 2D/2D Bi5FeTi3O15/g-C3N4 heterojunction for enhanced photocatalysis: mediator-induced interfacial charge transfer and mechanism insights. ACS Appl. Mater. Interfaces 11, 31.
Wang, M., Ye, M., Iocozzia, J., Lin, C., Lin, Z., 2016. Plasmon-mediated solar energy conversion via photocatalysis in noble metal/semiconductor composites. Adv. Sci. 3 (6), 1600024.
Wang, W., Zeng, Z., Zeng, G., Zhang, C., Xiao, R., Zhou, C., Xiong, W., Yang, Y., Lei, L., Liu, Y., Huang, D., Cheng, M., Yang, Y., Fu, Y., Luo, H., Zhou, Y., 2019c. Sulfur doped carbon quantum dots loaded hollow tubular g-C3N4 as novel photocatalyst for destruction of Escherichia coli and tetracycline degradation under visible light. Chem. Eng. J. 378, 122132.
Wang, W., Zhou, C., Yang, Y., Zeng, G., Zhang, C., Zhou, Y., Yang, J., Huang, D., Wang, H., Xiong, W., Li, X., Fu, Y., Wang, Z., He, Q., Jia, M., Luo, H., 2021. Carbon nitride based photocatalysts for solar photocatalytic disinfection, can we go further? Chem. Eng. J. 404, 126540.
Wang, X., Yin, R., Zeng, L., Zhu, M., 2019d. A review of graphene-based nanomaterials for removal of antibiotics from aqueous environments. Environ. Pollut. 253, 100–110.
Wang, Y., Balbuena, P.B., 2005. Potential energy surface profile of the oxygen reduction reaction on a Pt cluster: adsorption and decomposition of OOH and H2O2. J. Chem. Theory Comput. 1 (5), 935–943.
Wang, Y., Cao, D., Liu, M., Zhao, X., 2017. Insights into heterogeneous catalytic activation of peroxymonosulfate by Pd/g-C3N4: the role of superoxide radical and singlet oxygen. Catal. Commun. 102, 85–88.
Wu, B., Kuang, Y., Zhang, X., Chen, J., 2011. Noble metal nanoparticles/carbon nanotubes nanohybrids: Synthesis and applications. Nano Today 6 (1), 75–90.
Wu, M., Ding, T., Wang, Y., Zhao, W., Xian, H., Tian, Y., Zhang, T., Li, X., 2020. Rational construction of plasmon Au assisted ferroelectric-BaTiO3/Au/g-C3N4 Z-scheme system for efficient photocatalysis. Catal. Today 355, 311–318.
Wu, Q., Zhang, C., Arai, M., Zhang, B., Shi, R., Wu, P., Wang, Z., Liu, Q., Liu, K., Lin, W., Cheng, H., Zhao, F., 2019a. Pt/TiH2 catalyst for ionic hydrogenation via stored hydrides in the presence of gaseous H2. ACS Catal. 9 (7), 6425–6434.
Wu, S.M., Yang, X.Y., Janiak, C., 2019b. Confinement effects in zeolite-confined noble metals. Angew. Chem. Int. Ed. 58 (36), 12340–12354.
Wu, W., Liao, L., Zhang, S., Zhou, J., Xiao, X., Ren, F., Sun, L., Dai, Z., Jiang, C., 2013. Non-centrosymmetric Au-SnO2 hybrid nanostructures with strong localization of plasmonic for enhanced photocatalysis application. Nanoscale 5 (12), 5628–5636.
Xie, S., Yuan, S., Liao, P., Jia, M., Wang, Y., 2015. Pd-catalytic hydrodechlorination of chlorinated hydrocarbons in groundwater using H2 produced by a dual-anode system. Water Res. 86, 74–81.
Xie, Y.S., Zhang, N., Tang, Z.R., Anpo, M., Xu, Y.J., 2018. Tip-grafted Ag-ZnO nanorod arrays decorated with Au clusters for enhanced photocatalysis. Catal. Today 340, 121–127.
Xiong, Z., Zhang, L.L., Ma, J., Zhao, X.S., 2010. Photocatalytic degradation of dyes over graphene–gold nanocomposites under visible light irradiation. Chem. Commun. 46 (33), 6099–6101.
Xu, S., Carter, E.A., 2019. Theoretical insights into heterogeneous (photo) electrochemical CO_2 reduction. Chem. Rev. 119 (11), 6631–6669.
Xu, T., Zheng, H., Zhang, P., 2020. Isolated Pt single atomic sites anchored on nanoporous TiO2 film for highly efficient photocatalytic degradation of low concentration toluene. J. Hazard. Mater. 388, 121746.
Yamamoto, T., Takenaka, S., Tanaka, T., Baba, T., 2009. Stability of silver cluster in zeolite A and Y catalysts. J. Phys.: Conf. Ser. 190, 012171.
Yan, J., Wu, G., Guan, N., Li, L., 2013. Synergetic promotion of the photocatalytic activity of TiO2 by gold deposition under UV–visible light irradiation. Chem. Commun. 49.
Yan, Y., Yu, H., Zhang, K., Sun, M., Zhang, Y., Wang, X., Wang, S., 2016. Dual-emissive nanohybrid of carbon dots and gold nanoclusters for sensitive determination of mercuric ions. Nano Res. 9 (7), 2088–2096.
Yang, H., Ye, S., Zeng, Z., Zeng, G., Tan, X., Xiao, R., Wang, J., Song, B., Du, L., Qin, M., Yang, Y., Xu, F., 2020a. Utilization of biochar for resource recovery from water: a review. Chem. Eng. J. 397, 125502.
Yang, L., Gao, P., Lu, J., Guo, W., Zhuang, Z., Wang, Q., Li, W., Feng, Z., 2020b. Mechanism analysis of Au, Ru noble metal clusters modified on TiO2 (101) to intensify overall photocatalytic water splitting. RSC Adv. 10 (35), 20654–20664.
Yang, Q., Xu, Q., Jiang, H.L., 2017. Metal-organic frameworks meet metal nanoparticles: synergistic effect for enhanced catalysis. Chem. Soc. Rev. 46 (15), 4774–4808.
Yang, X., Tian, P.-F., Zhang, C., Deng, Y.-q, Xu, J., Gong, J., Han, Y.-F., 2013. Au/carbon as Fenton-like catalysts for the oxidative degradation of bisphenol A. Appl. Catal. B: Environ. 134–135, 145–152.
Yang, X.-j, Tian, P.-f, Wang, H.-l, Xu, J., Han, Y.-f, 2016. Catalytic decomposition of H2O2 over a Au/carbon catalyst: a dual intermediate model for the generation of hydroxyl radicals. J. Catal. 336, 126–132.
Yang, Y., Zeng, Z., Zeng, G., Huang, D., Xiao, R., Zhang, C., Zhou, C., Xiong, W., Wang, W., Cheng, M., 2019a. Ti3C2 Mxene/porous g-C3N4 interfacial Schottky junction for boosting spatial charge separation in photocatalytic H2O2 production. Appl. Catal. B: Environ., 117956
Yang, Y., Zeng, Z., Zeng, G., Huang, D., Xiao, R., Zhang, C., Zhou, C., Xiong, W., Wang, W., Cheng, M., Xue, W., Guo, H., Tang, X., He, D., 2019b. Ti3C2 Mxene/porous g-C3N4 interfacial Schottky junction for boosting spatial charge separation in photocatalytic H2O2 production. Appl. Catal. B: Environ. 258, 117956.
Yang, Y., Zhang, C., Huang, D., Zeng, G., Huang, J., Lai, C., Zhou, C., Wang, W., Guo, H., Xue, W., Deng, R., Cheng, M., Xiong, W., 2019c. Boron nitride quantum dots decorated ultrathin porous g-C3N4: intensified exciton dissociation and charge transfer for promoting visible-light-driven molecular oxygen activation. Appl. Catal. B: Environ. 245, 87–99.
Yang, Y., Li, X., Zhou, C., Xiong, W., Zeng, G., Huang, D., Zhang, C., Wang, W., Song, B., Tang, X., Li, X., Guo, H., 2020a. Recent advances in application of graphitic carbon nitride-based catalysts for degrading organic contaminants in water through advanced oxidation processes beyond photocatalysis: a critical review. Water Res. 184, 116200.
Yang, Y., Zeng, G., Huang, D., Zhang, C., He, D., Zhou, C., Wang, W., Xiong, W., Li, X., Li, B., Dong, W., Zhou, Y., 2020b. Molecular engineering of polymeric carbon nitride for highly efficient photocatalytic oxytetracycline degradation and H2O2 production. Appl. Catal. B: Environ. 272, 118970.
Yang, Y., Zeng, G., Huang, D., Zhang, C., He, D., Zhou, C., Wang, W., Xiong, W., Song, B., Yi, H., Ye, S., Ren, X., 2020c. In Situ Grown Single-Atom Cobalt on Polymeric Carbon Nitride with Bidentate Ligand for Efficient Photocatalytic Degradation of Refractory Antibiotics. Small 16 (29), 2001634.
Ye, F., Li, H., Yu, H., Chen, S., Quan, X., 2018. Constructing BiVO4-Au@CdS photocatalyst with energic charge-carrier-separation capacity derived from facet induction and Z-scheme bridge for degradation of organic pollutants. Appl. Catal. B: Environ. 227, 258–265.
Ye, S., Yan, M., Tan, X., Liang, J., Zeng, G., Wu, H., Song, B., Zhou, C., Yang, Y., Wang, H., 2019a. Facile assembled biochar-based nanocomposite with improved graphitization for efficient photocatalytic activity driven by visible light. Appl. Catal. B: Environ. 250, 78–88.

Ye, S., Zeng, G., Wu, H., Liang, J., Zhang, C., Dai, J., Xiong, W., Song, B., Wu, S., Yu, J., 2019b. The effects of activated biochar addition on remediation efficiency of co-composting with contaminated wetland soil. Resour. Conserv. Recycl. 140, 278–285.
Ye, S., Zeng, G., Tan, X., Wu, H., Liang, J., Song, B., Tang, N., Zhang, P., Yang, Y., Chen, Q., Li, X., 2020. Nitrogen-doped biochar fiber with graphitization from Boehmeria nivea for promoted peroxymonosulfate activation and non-radical degradation pathways with enhancing electron transfer. Appl. Catal. B: Environ. 269, 118850.
Yen, C.W., Mahmoud, M.A., El-Sayed, M.A., 2009. Photocatalysis in gold nanocage nanoreactors. J. Phys. Chem. A 113 (16), 4340–4345.
Yi, H., Yan, M., Huang, D., Zeng, G., Lai, C., Li, M., Huo, X., Qin, L., Liu, S., Liu, X., Li, B., Wang, H., Shen, M., Fu, Y., Guo, X., 2019. Synergistic effect of artificial enzyme and 2D nano-structured Bi2WO6 for eco-friendly and efficient biomimetic photocatalysis. Appl. Catal. B: Environ. 250, 52–62.
Yu, C., Cao, F., Li, G., Wei, R., Yu, J.C., Jin, R., Fan, Q., Wang, C., 2013. Novel noble metal (Rh, Pd, Pt)/BiOX(Cl, Br, I) composite photocatalysts with enhanced photocatalytic performance in dye degradation. Sep. Purif. Technol. 120, 110–122.
Yu, E., Li, J., Chen, J., Chen, J., Hong, Z., Jia, H., 2020a. Enhanced photothermal catalytic degradation of toluene by loading Pt nanoparticles on manganese oxide: photoactivation of lattice oxygen. J. Hazard. Mater. 388, 121800.
Yu, H., Wang, X., Sun, H., Huo, M., 2010. Photocatalytic degradation of malathion in aqueous solution using an Au–Pd–TiO2 nanotube film. J. Hazard. Mater. 184 (1), 753–758.
Yu, J., Lee, T.I., Misra, M., 2018. Synergetic impact of surface plasmon hot electron and CuS nanolayer of CuS/Au/ZnO core-shell nanorods for the degradation of toxic pollutant. J. Ind. Eng. Chem. 66, 468–477.
Yu, X., Wang, J., Fu, X., Meng, H., Zhu, Y., Zhang, Y., 2020b. Construction of Z-scheme SrTiO3/Ag/Ag3PO4 photocatalyst with oxygen vacancies for highly efficient degradation activity towards tetracycline. Sep. Purif. Technol. 241, 116718.
Yu, Y., Chen, Z., Guo, Z., Liao, Z., Yang, L., Wang, J., Chen, Z., 2015. Removal of refractory contaminants in municipal landfill leachate by hydrogen, oxygen and palladium: a novel approach of hydroxyl radical production. J. Hazard. Mater. 287, 349–355.
Yuan, N., Majeed, M.H., Bajnóczi, É.G., Persson, A.R., Wallenberg, L.R., Inge, A.K., Heidenreich, N., Stock, N., Zou, X., Wendt, O.F., Persson, I., 2019. In situ XAS study of the local structure and oxidation state evolution of palladium in a reduced graphene oxide supported Pd(ii) carbene complex during an undirected C–H acetoxylation reaction. Catal. Sci. Technol. 9 (8), 2025–2031.
Yuan, S., Fan, Y., Zhang, Y., Tong, M., Liao, P., 2011. Pd-catalytic in situ generation of H2O2 from H2 and O2 produced by water electrolysis for the efficient electro-Fenton degradation of rhodamine B. Environ. Sci. Technol. 45 (19), 8514–8520.
Zeng, H., Zhao, X., Zhao, F., Park, Y., Sillanpää, M., 2020. Accelerated Fe3+/Fe2+ cycle using atomic H* on Pd/Al2O3: a novel mechanism for an electrochemical system with particle electrode for iron sludge reduction in the Fe2+/peroxydisulfate oxidation process. Chem. Eng. J. 382, 122972.
Zhang, C., He, D., Fu, S., Zeng, G., Zhou, Y., 2021a. Silver iodide decorated ZnSn(OH)6 hollow cube: room-temperature preparation and application for highly efficient photocatalytic oxytetracycline degradation. Chem. Eng. J. 421, 129810.
Zhang, C., Tian, S., Qin, F., Yu, Y., Luo, H., 2021b. Catalyst-free activation of permanganate under visible light irradiation for sulfamethazine degradation: experiments and theoretical calculation. Water Res. 194 (7), 116915.
Zhang, F., Zhu, Y., Lin, Q., Zhang, L., Zhang, X., Wang, H., 2021c. Noble-metal single-atoms in thermocatalysis, electrocatalysis, and photocatalysis. Energy Environ. Sci. 14 (5), 2954–3009.
Zhang, H., Huang, H., Ming, H., Li, H., Zhang, L., Liu, Y., Kang, Z., 2012. Carbon quantum dots/Ag3PO4 complex photocatalysts with enhanced photocatalytic activity and stability under visible light. J. Mater. Chem. 22 (21), 10501–10506.
Zhang, J., Huang, B., Shao, Q., Huang, X., 2018a. Highly active, selective, and stable direct H2O2 generation by monodispersive Pd–Ag nanoalloy. ACS Appl. Mater. Interfaces 10 (25), 21291–21296.
Zhang, J., Shao, Q., Zhang, Y., Bai, S., Feng, Y., Huang, X., 2018b. Promoting the direct H2O2 generation catalysis by using hollow Pd–Sn intermetallic nanoparticles. Small 14 (16), 1703990.
Zhang, N., Ye, C., Yan, H., Li, L., He, H., Wang, D., Li, Y., 2020. Single-atom site catalysts for environmental catalysis. Nano Res. 13, 3165–3182.
Zhang, Q., Chen, S., Wang, H., Yu, H., 2018c. Exquisite enzyme-Fenton biomimetic catalysts for hydroxyl radical production by mimicking an enzyme cascade. ACS Appl. Mater. Interfaces 10 (10), 8666–8675.
Zhang, S., Ren, F., Wu, W., Zhou, J., Sun, L., Xiao, X., Jiang, C., 2014. Size effects of Ag nanoparticles on plasmon-induced enhancement of photocatalysis of Ag-α-Fe2O3 nanocomposites. J. Colloid Interface Sci. 427, 29–34.
Zhang, W., Li, G., Liu, H., Chen, J., Ma, S., An, T., 2019. Micro/nano-bubble assisted synthesis of Au/TiO2@CNTs composite photocatalyst for photocatalytic degradation of gaseous styrene and its enhanced catalytic mechanism. Environ. Sci.: Nano 6 (3), 948–958.
Zhang, X., Tang, A., Jia, Y., Wang, Y., Wang, H., Zhang, S., 2017. Enhanced visible-light-driven photocatalytic performance of Ag/AgGaO2 metal semiconductor heterostructures. J. Alloy. Compd. 701, 16–22.
Zhang, Z., Jiang, X., Liu, B., Guo, L., Lu, N., Wang, L., Huang, J., Liu, K., Dong, B., 2018d. IR-driven ultrafast transfer of plasmonic hot electrons in nonmetallic branched heterostructures for enhanced H2 generation. Adv. Mater. 30 (9), 1705221.
Zhao, P., Feng, X., Huang, D., Yang, G., Astruc, D., 2015. Basic concepts and recent advances in nitrophenol reduction by gold- and other transition metal nanoparticles. Coord. Chem. Rev. 287, 114–136.
Zhao, Q., Liu, L., Liu, R., Zhu, L., 2018. PdCu nanoalloy immobilized in ZIF-derived N-doped carbon/graphene nanosheets: alloying effect on catalysis. Chem. Eng. J. 353, 311–318.
Zhao, W., Xie, L., Zhang, M., Ai, Z., Xi, H., Li, Y., Shi, Q., Chen, J., 2016. Enhanced photocatalytic activity of all-solid-state g-C3N4/Au/P25 Z-scheme system for visible-light-driven H2 evolution. Int. J. Hydrog. Energy 41 (15), 6277–6287.
Zhao, X., Yang, H., Cui, Z., Yi, Z., Yu, H., 2019. Synergistically enhanced photocatalytic performance of Bi4Ti3O12 nanosheets by Au and Ag nanoparticles. J. Mater. Sci.: Mater. Electron. 30 (14), 13785–13796.
Zheng, Z., Murakami, N., Liu, J., Teng, Z., Zhang, Q., Cao, Y., Cheng, H., Ohno, T., 2020. Development of plasmonic photocatalyst by site-selective loading of bimetallic nanoparticles of Au and Ag on titanium(IV) oxide. ChemCatChem 12 (14), 3783–3792.
Zhong, Y., Peng, C., He, Z., Chen, D., Jia, H., Zhang, J., Ding, H., Wu, X., 2021. Interface engineering of heterojunction photocatalysts based on 1D nanomaterials. Catal. Sci. Technol. 11 (1), 27–42.
Zhou, C., Wang, S., Zhao, Z., Shi, Z., Yan, S., Zou, Z., 2018. A facet-dependent schottky-junction electron shuttle in a BiVO4{010}–Au–Cu2O Z-scheme photocatalyst for efficient charge separation. Adv. Funct. Mater. 28 (31), 1801214.
Zhou, C., Zeng, G., Huang, D., Luo, Y., Cheng, M., Liu, Y., Xiong, W., Yang, Y., Song, B., Wang, W., Shao, B., Li, Z., 2020a. Distorted polymeric carbon nitride via carriers transfer bridges with superior photocatalytic activity for organic pollutants oxidation and hydrogen production under visible light. J. Hazard. Mater. 386, 121947.
Zhou, H., Zhang, H., He, Y., Huang, B., Zhou, C., Yao, G., Lai, B., 2021. Critical review of reductant-enhanced peroxide activation processes: Trade-off between accelerated Fe3+/Fe2+ cycle and quenching reactions. Appl. Catal. B: Environ. 286, 119900.
Zhou, X., Zeng, Z., Zeng, G., Lai, C., Xiao, R., Liu, S., Huang, D., Qin, L., Liu, X., Li, B., Yi, H., Fu, Y., Li, L., Zhang, M., Wang, Z., 2020b. Insight into the mechanism of persulfate activated by bone char: unraveling the role of functional structure of biochar. Chem. Eng. J. 401, 126127.
Zhu, S., Ho, S.-H., Jin, C., Duan, X., Wang, S., 2020. Nanostructured manganese oxides: natural/artificial formation and their induced catalysis for wastewater remediation. Environ. Sci. Nano 7 (2), 368–396.
Zhu, W., Chen, S., 2020. Recent progress of single-atom catalysts in the electrocatalytic reduction of oxygen to hydrogen peroxide. Electroanalysis 32 (12), 2591–2602.
Zhu, Y., Zhao, X., Cao, D., Wang, Y., Yanbin, 2017. Peroxymonosulfate enhanced visible light photocatalytic degradation bisphenol A by single-atom dispersed Ag mesoporous g-C3N4 hybrid. Appl. Catal. B. Environ. 211, 79–88.